frontiers | Frontiers in Earth Science

TYPE Review
PUBLISHED 14 November 2023
DOI 10.3389/feart.2023.1254309

OPEN ACCESS

EDITED BY
Mathias Bavay,
WSL Institute for Snow and Avalanche Research SLF, Switzerland

REVIEWED BY
Scott L. Painter,
Oak Ridge National Laboratory (DOE), United States
Jannes Kordilla,
Spanish National Research Council (CSIC), Spain

*CORRESPONDENCE
Magdalena Diak,
mdiak@iopan.pl

RECEIVED 06 July 2023
ACCEPTED 23 October 2023
PUBLISHED 14 November 2023

CITATION
Diak M, Böttcher ME, Ehlert von Ahn CM, Hong W-L, Kędra M, Kotwicki L, Koziorowska-Makuch K, Kuliński K, Lepland A, Makuch P, Sen A, Winogradow A, Silberberger MJ and Szymczycha B (2023), Permafrost and groundwater interaction: current state and future perspective.
Front. Earth Sci. 11:1254309.
doi: 10.3389/feart.2023.1254309

Permafrost and groundwater interaction: current state and future perspective

Magdalena Diak[1]*, Michael Ernst Böttcher[2,3,4], Cátia Milene Ehlert von Ahn[2], Wei-Li Hong[5], Monika Kędra[1], Lech Kotwicki[1], Katarzyna Koziorowska-Makuch[1], Karol Kuliński[1], Aivo Lepland[6], Przemysław Makuch[1], Arunima Sen[7,8], Aleksandra Winogradow[1], Marc Jürgen Silberberger[1] and Beata Szymczycha[1]

[1]Institute of Oceanology Polish Academy of Sciences, Sopot, Poland, [2]Leibniz Institute for Baltic Sea Research (IOW), Geochemistry and Isotope Biogeochemistry, Warnemünde, Germany, [3]Marine Geochemistry, University of Greifswald, Greifswald, Germany, [4]Interdisciplinary Faculty, University of Rostock, Rostock, Germany, [5]Department of Geological Sciences, Stockholm University, Stockholm, Sweden, [6]Geological Survey of Norway, Trondheim, Norway, [7]Department of Arctic Biology, The University Centre in Svalbard (UNIS), Longyearbyen, Norway, [8]Faculty of Biosciences and Aquaculture, Nord University, Bodø, Norway

This study reviews the available and published knowledge of the interactions between permafrost and groundwater. In its content, the paper focuses mainly on groundwater recharge and discharge in the Arctic and the Qinghai-Tibet Plateau. The study revealed that the geochemical composition of groundwater is site-specific and varies significantly within the depth of the aquifers reflecting the water-rock interactions and related geological history. All reviewed studies clearly indicated that the permafrost thaw causes an increase in groundwater discharge on land. Furthermore, progressing climate warming is likely to accelerate permafrost degradation and thus enhance hydrological connectivity due to increased subpermafrost groundwater flow through talik channels and higher suprapermafrost groundwater flow. In the case of submarine groundwater discharge (SGD), permafrost thaw can either reinforce or reduce SGD, depending on how much pressure changes affecting the aquifers will be caused by the loss of permafrost. Finally, this comprehensive assessment allowed also for identifying the lack of long-term and interdisciplinary *in situ* measurements that could be used in sophisticated computational simulations characterizing the current status and predicting groundwater flow and permafrost dynamics in the future warmer climate.

KEYWORDS

groundwater discharge, groundwater recharge, climate change, groundwater hydrochemistry, submarine groundwater discharge

1 Introduction

The Arctic, subarctic, and Qinghai-Tibet Plateau (QTP) zones are facing severe transformations as a result of climate change (Immerzeel et al., 2010; Rowland et al., 2010; Wu et al., 2013; Luo et al., 2019; Doloisio and Vanderlinden, 2020; Larsen et al., 2021). Warming occurs significantly faster in higher latitudes and QTP than elsewhere in the world (Jia et al., 1958; Khare and Khare, 1968; Flohn, 1980; Manabe et al., 1991; McBean et al., 2005;

Turner et al., 2007). The Arctic region experiences the so-called "Arctic amplification," which is a term to describe intense warming, up to three times faster than the global average (Shijin et al., 2023). Global warming contributes to a significant reduction in the thickness of the permafrost (Box et al., 2019) which occupies approximately 15 x 10^6 km^2 (15%) of the Earth's land surface (Obu, 2021). The permafrost thaw makes previously immobile organic matter, inorganic nutrients, metals, and other substances, including those of anthropogenic origin, accessible for dislocation and migration into aquatic environments. Permafrost thaw can provide substantial feedback to climate by triggering and transporting prior trapped carbon within the permafrost and leading to the release of carbon dioxide (CO_2) and methane (CH_4) and further climate warming (Schuur et al., 2015). The degradation of permafrost led to the reorganisation of vegetation, water storage and flow paths, and patterns of organic carbon accumulation; however, most studies have focused only on investigating the release of selected dissolved chemical constituents. Furthermore, permafrost effectively controls and affects hydrological processes (Ensom et al., 2020). Hydrological shifts associated with climate change and permafrost thaw create serious uncertainty when projecting fluxes of water, energy, sediments, and solutes to fluvial and marine ecosystems (Sjöberg et al., 2021; Bring et al., 2016; Hinzman et al., 2005). Transfer of carbon and nutrients through groundwater in permafrost terrain to surface waters will likely alter the productivity of aquatic ecosystems, driving bottom-up shifts in food web dynamics (Creed et al., 2018; Kendrick et al., 2018). Changes in groundwater discharge associated with permafrost thaw can also alter the thermal regime of surface waters, which functions as a primary control of ecosystem and organismal processes. Furthermore, groundwater movement from land to sea can denote a major source of freshwater and nutrients for coastal ecological and biogeochemical processes polar and subpolar (Connolly et al., 2020). However, there is little information on groundwater-permafrost interactions and their influence on the functioning of the environment. Previous reviews (e.g., Walvoord and Kurylyk, 2016) focused primarily on physical aspects and hydrological modelling in permafrost environments. A synthesis of biogeochemistry of the major groundwater types in permafrost regions, with emphasis on the flow of groundwater into the marine/terrestrial environment and solute concentrations is still missing.

In this study, our objective is to synthesize existing knowledge on the role of groundwater circulation in the permafrost regions of the Northern Hemisphere, including the highly complex and heterogenic mountainous terrain of QTP with a focus on groundwater biogeochemistry and discharge (Figure 1). In addition, we determine the potential climate-driven dynamic responses associated with groundwater flow and solute fluxes and identify knowledge gaps and future research needs.

1.1 Principal definitions

In a glossary, prepared by Everdingen. (1998) and approved by the International Permafrost Association (IPA), permafrost is defined as perennially frozen ground (soil or rock and including ice and organic material) with temperatures near or below 0°C for at least two consecutive years (Table 1). Based on this definition, water does not have to be frozen, may be partially frozen or even unfrozen due to freezing-point depression. As a consequence, all perennially frozen ground is perceived as permafrost, whereas in the opposite direction of the theorem, it is not always true. Therefore, permafrost should not be considered permanent, since it is not resistant to climate changes that can lead to an increase in ground temperature above 0°C. Unfrozen permafrost exists, for example, in regions of the continental shelf of the Arctic Sea in northern Alaska and Siberia due to the intrusion of salt from sea water, which lowers the freezing temperature. An analogous situation is observed under massive glaciers, where elevated pressure of ice cover prevents water from freezing, despite temperatures lower than 0°C and sometimes even below −60°C. Furthermore, the type of ground material may also strongly affect the phase transition process of water and therefore contribute to only partial freeze of water in permafrost. Fine-grained soil materials, such as bentonite, clay, and loam, are examples of these kinds of medium. Additionally, the definition of permafrost and its full understanding requires determining its water content. Permafrost devoid of water in both liquid and ice forms is called dry permafrost. Everdingen. (1998) presented a definition that included the presence of an insignificant amount of moisture in the form of interfacial water. However, this concept is not so precise because ice by definition is also dry, and appropriate comprehension of water as a triphase substance is more complex (Dobinski, 2011). Typical classification is based on the percentage coverage of the area with permafrost. According to this, the following types of permafrost can be recognised, continuous permafrost, and discontinuous permafrost (Figure 2). Permafrost is defined as continuous permafrost if the permafrost covers more than 90% of the ground. Based on the percentage of occupied area by permafrost, several subtypes can be differentiated in case of discontinuous permafrost, such as extensive discontinuous permafrost (65%–90%), intermediate discontinuous permafrost (35%–65%), sporadic discontinuous permafrost (10%–35%) and isolated patches (0%–10%) (Table 1). In addition, particular regions of discontinuous permafrost are entirely encircled by unfrozen ground. Another important issue in continuous permafrost environment is microtopography which can control the water balance and initiate terrestrial water drainage and discharge to the surface (Liljedahl et al., 2012; Liljedahl et al., 2016; Painter et al., 2016; Harp et al., 2020; Nitzbon et al., 2020; Painter et al., 2023). Ice-wedge polygons are examples of these kind of feature and commonly occur in polygonal tundra that occupies around 30% of the Arctic land. Ice-wedge polygons are formed during repeated cycles of thermal contraction cracking and water infiltration (Liljedahl et al., 2016). We distinguish main two types of ice-wedge polygons: low-centred and high-centred polygons. In contrast to high-centred polygons, low-centred polygons are characterized by raised-edge with frequently inundated center (Liljedahl et al., 2016). During the thermokarst process low-centred ice-wedge polygons undergo transformation into high-centred ice-wedge polygons and this causes severe changes in the water balance partitioning (Liljedahl et al., 2012). These features of lowland tundra have an effect on suprapermafrost groundwater seepage into surface-water drainage channels. Transport of nutrients through the shallow groundwater fluxes into surface is greatly affected by ice-wedge polygons (Helbig et al., 2013; Harp et al., 2020). Furthermore, surface surveys conducted and data collected

TABLE 1 Acronyms and definitions.

Term	Definition	References
Active layer	In the permafrost region, it is the upper layer of ground that undergoes seasonal thawing and freezing	Everdingen et al. (1998)
Aquitards	Geologic formation that allows groundwater to flow at a very slow rate from one adjacent aquifer to another	Celico (1986)
Continuous permafrost	When permafrost covers more than 90% of the area	Everdingen (1998)
Cryopegs	Perennially cryotic part of the unfrozen ground that is characterized by freezing-point depression	Everdingen (1998)
Cryotic taliks	Taliks with average annual temperatures below 0°C	Everdingen (1998)
DIC	Dissolved inorganic carbon	abbreviation
DIN	Dissolved inorganic nitrogen	abbreviation
DIP	Dissolved inorganic phosphorus	abbreviation
Discontinuous permafrost	This classification is sub-divided into several subtypes based on the percentage of area occupied by permafrost: extensive discontinuous permafrost (65%–90%), intermediate discontinuous permafrost (35%–65%), sporadic discontinuous permafrost (10%–35%), and isolated patches (0%–10%)	Everdingen (1998)
DOC	Dissolved organic carbon	abbreviation
DOM	Dissolved organic matter	abbreviation
Dry permafrost	Permafrost devoid of water in both liquid and ice forms	Everdingen (1998)
Groundwater discharge	Result of the groundwater-surface water interaction and is defined as the groundwater flow from the saturated zone to surface water	Lamontagne-Hallé et al. (2018)
Hydrochemical taliks	Cryotic taliks preserved by mineralized groundwater flow	Everdingen (1998)
Hydrothermal taliks	A noncryotic taliks with average annual temperatures maintained above 0 °C from heat transfer by groundwater flow	Everdingen (1998)
Ice-wedge polygon	periglacial landforms formed during thermal contraction cracking followed by water infiltration	Hawkswell (2018)
Icing blisters	Mounds created during seasonal freezing of groundwater flowing out of a spring under pressure	Michel (2005)
Intrapermafrost groundwater	Exists within the permafrost and is defined as water present in unfrozen zones such as taliks or cryopegs	Everdingen (1998)
Microtopography	here, small features of permafrost wetlands that strongly affects water balance and active layer depth	Grant et al., 2017
Non-cryotic taliks	Taliks with average annual temperatures above 0°C	Everdingen (1998)
Permafrost	Frozen ground (soil or rock, including ice and organic material) with temperatures near or below 0 °C for at least two consecutive years. However, water may be partially frozen or even unfrozen due to freezing-point depression. Glacier ice, ice thaws, and artificially created perennially frozen ground are not referred to as permafrost	Everdingen, 1998; Dobiński, 2011
POC	Particulate organic carbon	abbreviation
SGD	Submarine groundwater discharge in the form of springs or seeps is a specific type of hydrological process that is commonly observed on the sea floor. SGD may also be diffusively released	Burnett et al. (2003)
SOC	Soil organic carbon	abbreviation
Subpermafrost groundwater	Appears in the noncryotic ground below the bottom of permafrost	Everdingen (1998)
Subsea permafrost	Permafrost located beneath the sea bottom	Everdingen (1998)
Suprapermafrost groundwater	Water in unfrozen ground above the top of the permafrost layer and is present in the active layer, between the active layer and the permafrost, and in taliks below rivers and lakes	Everdingen (1998)
Talik	A layer or area of unfrozen ground within the permafrost that has existed for more than a year. Taliks are formed during regional thermal, hydrological, hydrogeological, or hydrochemical anomalies. Some taliks may be vulnerable to seasonal freeze processes. Taliks may serve as a connection between water from different layers of permafrost and facilitate groundwater discharge into the surface, terrestrial and marine systems	Everdingen (1998)
QTP	Qinghai-Tibet Plateau	abbreviation

form remote sensing technique revealed that dramatic alteration of polygonal tundra occurred over the last decades (Liljedahl et al., 2016). As a result, more than 90% of the examined territory in the Arctic region revealed extensive widespread ice-wedge degradation. Therefore, more attention should be paid for these geomorphological features in low gradient arctic wetlands.

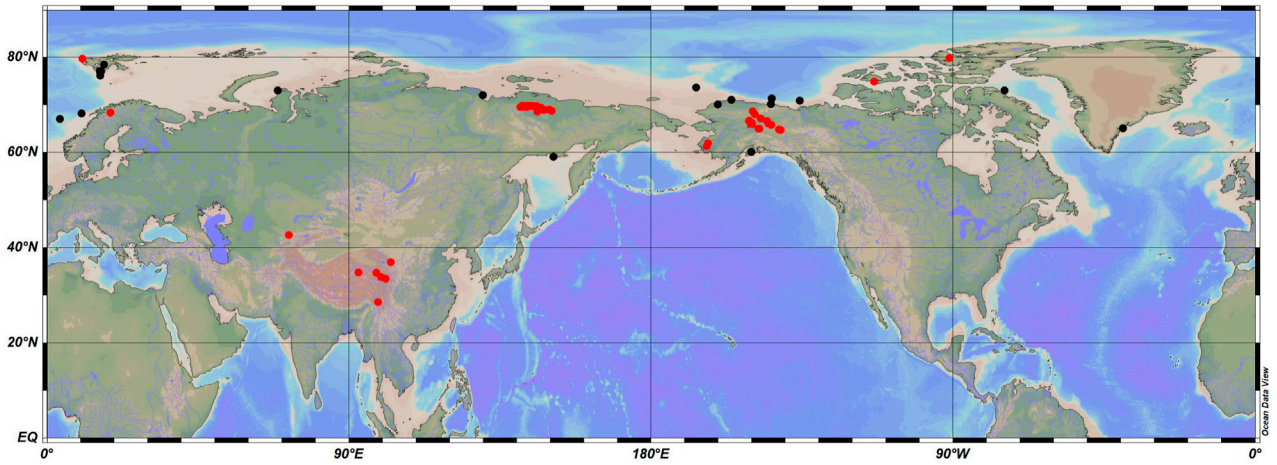

FIGURE 1
Map with the localities in the permafrost regions where groundwater discharge has been estimated or measured (black dots, groundwater discharge into the marine environment; red dots, groundwater discharge into the terrestrial environment.

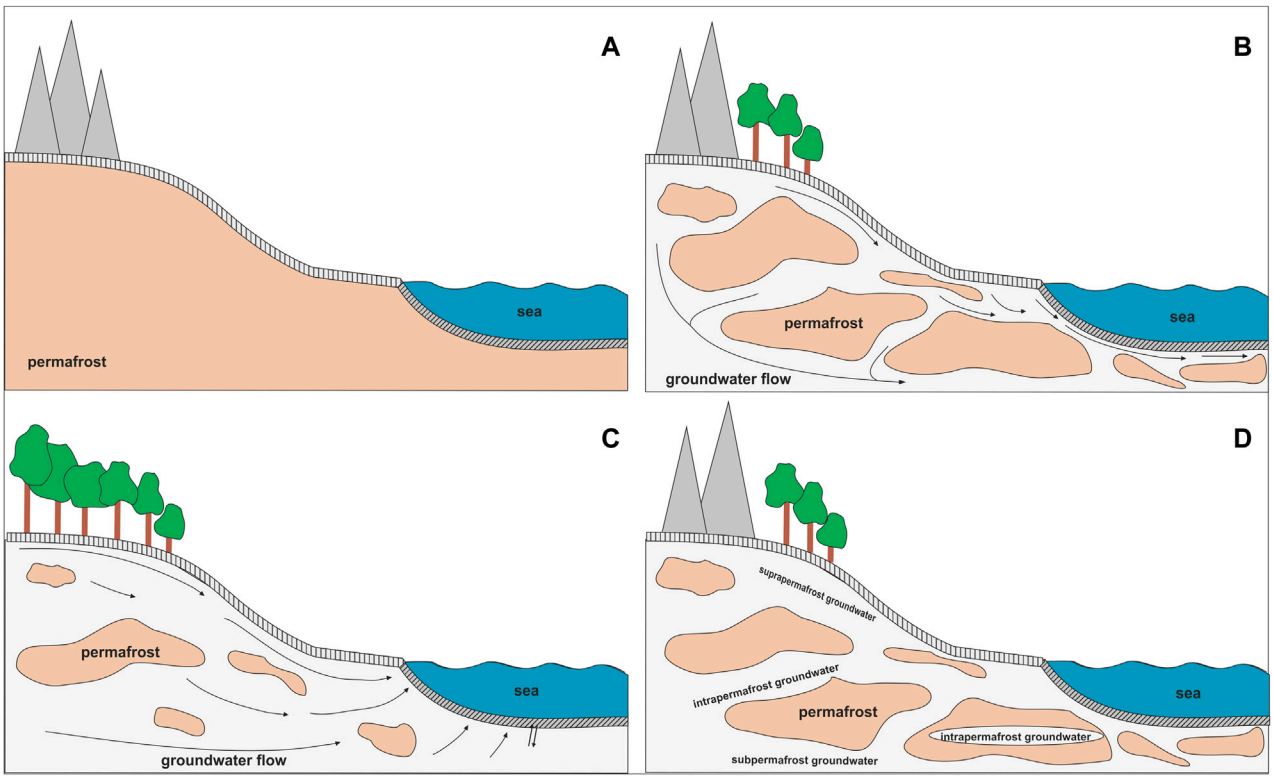

FIGURE 2
Types of permafrost: **(A)** continuous, **(B)** discontinuous, **(C)** sporadic, and **(D)** groundwater in permafrost region.

Besides types of permafrost, we can distinguish subsea permafrost, which occurs beneath the sea bottom. Another very important and often used term is "talik," which is a layer or area of unfrozen ground that has existed for more than a year (Table 1). Talik is formed during regional thermal, hydrological, hydrogeological, or hydrochemical anomalies. Some taliks may be vulnerable to seasonal freeze processes. Two types of talik can be distinguished based on their temperatures, namely, non-cryotic (for taliks with temperatures above 0°C) or cryotic (for taliks with temperatures below 0°C). Taliks may serve as a connection between water from different layers of permafrost and facilitate groundwater discharge into surface, terrestrial, and marine systems. In the permafrost environment,

TABLE 2 Chemical composition of supra-, sub- and intra-permafrost groundwater (n.d.—no date).

No.	Region	Predominant water types	HCO_3^- (mg/L)	Ca^{2+} (mg/L)	Mg^{2+} (mg/L)	SO_4^{2-} (mg/L)	TDS (mg/L)	Cl^-(mg/L)	Na^+ (mg/L)	Aquifer lithologies/soil types	References
Suprapermafrost groundwater											
1	Hulugou catchment in the northeast QTP	$HCO_3^- \cdot Ca^{2+}$	294	72	15	10	265	6	9	calcite. Weathered sandstone with fractures	Ma et al., 2017, Hu et al., 2019
2	Fish Hole (Canada), Yukon North Slope; Big Fish River—shallow suprapermafrost groundwater	$Ca^{2+} \cdot SO_4^{2-}$	195	81.3	15	199	700	131	112	gypsum; limestone bedrock	Clark et al. (2001)
3	Fish Hole (Canada), Yukon North Slope; Big Fish River—deeper suprapermafrost groundwater	$Ca^{2+} \cdot HCO_3^-$	11–159	6–57	0.4–2.6	0.9–7.4	20–221	0.1–0.7	0.1–0.4	gypsum; limestone bedrock	Clark et al. (2001)
4	Lena River in central Yakutia, Yakutsk eastern Siberia	$Mg^{2+} \cdot Ca^{2+} \cdot HCO_3^-$	72–139	21–31	8.1–11.7	9.1–29.0	35–200	25.0–27.4	11.2–27.0	seasonally thawing layer	Pavlova et al., 2016
5	Brattegg River drainage basin, Spitsbergen (Svalbard)	$HCO_3^- \cdot Mg^{2+} \cdot Ca^{2+}$ and $HCO_3^- \cdot Ca^{2+} \cdot Mg^{2+}$	16–47	1.4–8.1	1.4–6.1	1.6–10	>130	1.5–4.0	2.2–3.9	proterozoic crystalline rocks; Quaternary clastic formations	Marszałek et al., 2013
6	southern Spitsbergen (Svalbard), Finsterwalderbreen	$SO_4^{2-} \cdot Mg^{2+} \cdot Ca^{2+}$	109.8	440	480	2208	no data	no data	no data	Limestone and dolomite	Cooper et al. (2002)
7	Hornsund, Spitsbergen (Svalbard)	$HCO_3^- \cdot Cl^- \cdot Ca^{2+}$ and $Cl^- \cdot HCO_3^- \cdot Ca^{2+}$, $HCO_3^- \cdot SO_4^{2-} \cdot Ca^{2+}$	12–78	2.3–25	0.7–4.1	1–15	20–150	5.5–10.8	1.7–6.0	carbonate rocks	Olichwer et al. (2013)
8	Hornsund, Spitsbergen (Svalbard), sample from melt water	$HCO_3^- \cdot Cl^- \cdot Ca^{2+}$	31	7.1	2.6	4.2	40–50	9	3.9	non carbonate rocks	Olichwer et al. (2013)
9	Hornsund, Spitsbergen (Svalbard), Karst spring	$HCO_3^- \cdot Ca^{2+} \cdot SO_4^{2-} \cdot Cl^-$	79	25.3	4.1	15.1	100–150	10.8	6	carbonate rocks	Olichwer et al. (2013)
10	Yukon Territory (Canada)	no data	no data	no data	no data	4.3–391	no data	no data	no data	sedimentary rocks, meta-sediments	van Stempvoort et al. (2023)
11	Southwestern part of Spitsbergen (Svalbard)	$HCO_3^- \cdot Cl^- \cdot Na^+ \cdot Mg^{2+} \cdot Ca^{2+}$	4.6–49.1	1.2–10	1.2–5.7	0.3–6.7	16–157	5–25.5	2.1–8.2	metamorphic rocks	Rysiukiewicz et al., 2023
12	QTP	$HCO_3^- \cdot Ca^{2+}$, $HCO_3^- \cdot Ca^{2+} \cdot Mg^{2+}$, and $HCO_3^- \cdot Na^+$	no data	no data	no data	no data	100–300	no data	no data	no data	Cheng and Jin (2013)
Intrapermafrost groundwater											
13	Lena River in central Yakutia, Yakutsk eastern Siberia	$Mg^{2+} \cdot HCO_3^-$	606–650	12–19	29–80	0.3	890–1,044	29–135	108–250	water of under lake talik, Quaternary aquifer (sand–pebble deposits)—Middle Cambrian aquifer	Pavlova et al., 2016

(Continued on following page)

10.3389/feart.2023.1254309

TABLE 2 (*Continued*) Chemical composition of supra-, sub- and intra-permafrost groundwater (n.d.—no date).

No.	Region	Predominant water types	HCO_3^- (mg/L)	Ca^{2+} (mg/L)	Mg^{2+} (mg/L)	SO_4^{2-} (mg/L)	TDS (mg/L)	Cl^-(mg/L)	Na^+ (mg/L)	Aquifer lithologies/soil types	References
14	Hornsund, Spitsbergen (Svalbard)	HCO_3^- ·SO_4^{2-} ·Ca^{2+}·Mg^{2+}	137–195	16–85	14–40	20–200	110–700	42–140 L	30–110	no data	Olichwer et al. (2013)
15	Hulugou, QTP	Mg^{2+}·Ca^{2+}·HCO_3^-	834	205	96	4	1,059	106	221	silt clay with small gravel	Ma et al. (2017)
Subpermafrost groundwater											
16	Orvin Spring, Hornsund, Spitsbergen (Svalbard)	Cl^-·Na^+	62–79	14–15	7.5–10	21–31	187–228	46–49	32–36	no data	Olichwer et al. (2013)
17	Daldyn–Alakit, Siberia	SO_4^{2-}·Mg^{2+}·Ca^{2+}	330	13,000	7,000	340	380 (summer)—730 (late winter)	57,000	7,710–24420	Upper Cambrian aquifer	Alexeev and Alexeeva (2003)
18	Raudfjellet Spring, Hornsund, Spitsbergen (Svalbard)	Cl^-·HCO_3^-·Na^+·Ca^{2+}·Mg^{2+}	78	23	10	39–48	317–378	56	2	no data	Olichwer et al. (2013)
19	Central Yakutia, eastern Siberia	Cl^-·HCO_3^-·Na^+·Mg^{2+}	715	3.2	3.6	21	1,525	282	453	Middle Cambrian aquifer	Pavlova et al., 2016
20	Siberian Arctic	no data	no data	no data	no data	no data	10,000–30000	no data	no data	Metamorphic bedrock of pre-upper Cretaceous complexes	Charkin et al., 2017
21	QTP	Cl^-·Na^+ and Cl^-·HCO_3^-·Na^+·Ca^{2+}	no data	no data	no data	no data	more than 61% > 1,000	no data	no data	Triassic aquifer	Cheng and Jin (2013)
22	Hulugou catchment, QTP	HCO_3^-·SO_4^{2-}·Mg^{2+}·Ca^{2+}	238	47	23	65	303	18	23	no data	Ma et al. (2017)
23	Hulugou catchment, QTP	HCO_3^-·SO_4^{2-}·Mg^{2+}·Ca^{2+}	238–261	47–69	23–44	65–170	307–438	no data	no data	sandy gravel	Hu et al.,. 2018
24	Fish Hole (Canada); Cache Creek springs	Na^+·Cl^-(SO_4^{2-})	266–294	78–108	22–24	441–540	3,000–3,500	1,156–1,254	982–1,093	no data	Clark et al. (2001)
25	Fish Hole (Canada), Marine Shale seeps	Na^+·Cl^-(SO_4^{2-})	299–305	77–84	18–19	383–399	3,200	1,018–1,055	937–1,010	no data	Clark et al. (2001)

10.3389/feart.2023.1254309

several types of groundwater can be recognized, such as suprapermafrost groundwater, intrapermafrost groundwater, and subpermafrost groundwater (Figure 2D). Intrapermafrost groundwater exists within the permafrost and is defined as water present in unfrozen zones such as previously described taliks or cryopegs (the perennially cryotic part of the unfrozen ground that is characterized by freezing-point depression). Subpermafrost groundwater appears in the noncryotic ground below the bottom of permafrost, while suprapermafrost groundwater determines water above the top of the permafrost layer and occurs in the active layer, between the active layer and the permafrost, and in taliks below rivers and lakes. An active layer is made up of soil or rock and is a top layer of soil located above the permafrost table. Depending on the type of permafrost zone, the active layer predominantly reaches or does not reach the permafrost table in the continuous or discontinuous permafrost region, respectively. The active layer comprises the uppermost part of the permafrost and undergoes seasonal thawing and freezing in permafrost zone. The depth of the frozen layer may differ and reaches various levels relative to the permafrost table. The summary of definitions is presented in Table 1.

2 Composition of groundwater in permafrost areas

The general geochemical composition of groundwater and the concentration of solutes can provide information on the type of groundwater in the permafrost area. The type of groundwater can be differentiated within a depth of the aquifer and reflect the characteristics of the region. Furthermore, the chemical composition of groundwater changes as water moves and interacts with various lithologies (Boulding and Ginn, 2016). Various chemical (e.g., oxidation-reduction, dissolution, precipitation) and physical processes are taking place during an interaction between groundwater and environment, and its final product is mainly affected by lithology, water-rock interactions, flow paths, and residence time (Tóth, 1999; Kim et al., 2022). Based on the concentration of main ions such as HCO_3^-, Ca^{2+}, Mg^+, SO_4^{2-}, Cl^-, Na^+, groundwater can be roughly assigned to different types (supra-, intra-, or subpermafrost groundwater) and lithological and geological characteristics of the territory. For example, Herczeg and Edmunds. (2000) revealed that at the beginning of groundwater flow, the shallow part of the aquifer consists of atmospherically derived solutes. With time and ongoing interactions between rock and water, the chemical composition of groundwater begins to reflect the geological characteristics of the region (Table 2).

In general, the groundwater flow from suprapermafrost occurs in shallow aquifers and is usually characterised by the presence of carbonates with less influence of silicates. However, the subpermafrost groundwater flow that occurs below incoherent soil layers is dominated by minerals derived from rock weathering reactions (Herczeg and Edmunds, 2000).

2.1 Suprapermafrost groundwater

The chemical composition of suprapermafrost groundwater depends on many aspects such as topographic and geomorphological features, type of permafrost (continuous/discontinuous/sporadic), atmospheric conditions, physical rock properties, and groundwater flow dynamics (Marszałek and Wasik, 2013; Pokrovsky et al., 2015; Manasypov et al., 2020). In the Arctic and QTP, groundwater from the active layer of permafrost is characterised by low mineralisation values compared to intra- or sub-permafrost groundwater (Table 2). This is due to the short residence time of suprapermafrost groundwater in the comparatively well-permeable rock environment (Marszałek and Wasik, 2013). The suprapermafrost groundwater in the Hulugou catchment in the Heihe River region of the northeast QTP was found to be of the HCO_3^--Ca^{2+} type with low mineralisation value (Ma et al., 2017; Hu et al., 2019). The same suprapermafrost groundwater type was discovered in the continuous permafrost zone located at Fish Hole near Aklavik (Canada) (Clark et al., 2001). The origin of the suprapermafrost groundwater composition in Aklavik was meteoric water and active layer drainage (Clark et al., 2001). In the Heihe River region, calcium carbonate dissolution primarily regulated water ionic compositions. This assumption was supported by a strong relationship between [Ca^{2+} + Mg^{2+}] and [HCO_3^- + CO_3^{2-}] and negative saturation indices of calcite and dolomite saturation indices (Table 2) (Hu et al., 2019). In addition, the suprapermafrost groundwater had high pH values between 7.4–8.9 and the lowest value was probably due to high concentrations of dissolved organic acid from the shallow organic soil layer (Hu et al., 2019). It was also indicated in the eastern Alaskan Beaufort Sea coast that an active layer and shallow permafrost contain a large source of organic carbon and nitrogen that may induce the production of leachable DOM (Connoly et al., 2020). The content of OM in the soil of the Alaskan Beaufort Sea coast varied with depth and the highest amount was found in the surface layer where plant litter was also observed. The collected samples contained between 5% and 20% organic carbon and between 0.25% and 1.3% organic nitrogen, which are characteristic values for active layers of the tundra and upper permafrost soils (Connoly et al., 2020). The predominant water types of suprapermafrost groundwater in different regions such as Ulakhan Taryn Creek in Central Yakutia, eastern Siberia, or Brattegg River drainage basin in the Hornusnd region (Svalbard) (Table 2) were quite similar and consisted mainly of HCO_3^--Mg^{2+}-Ca^{2+} and HCO_3^--Ca^{2+}-Mg^{2+} ions (Marszałek and Wasik, 2013; Pavlova et al., 2016). The shallow groundwater in the southwestern part of Spitsbergen (Svalbard) showed a higher concentration of Cl^- than in the previous regions with a dominant HCO_3^- content (Rysiukiewicz et al., 2023). Presumably, the weathering of the silicates in metamorphic rock was the source of HCO_3^- ions. However, the aerosols of the Greenland Sea seem to be responsible for a greater contribution of Cl^- to groundwater composition, as they can be transported by precipitation (Rysiukiewicz et al., 2023). The Proglacial zone of Finsterwalderbreen (Spitsbergen, Norway) was an exception, and in this region relatively high concentrations of the main ions SO_4-Mg-Ca and Mg-Ca-HCO_3 were observed, often exceeding the values recorded in sub- and intra-permafrost groundwater (Cooper et al., 2002). It has been indicated that limestone and dolomite were responsible for a high concentration of DIC and Ca^{2+} in groundwater. Although oxidation of sulphides and secondary sulphate salts was an important source of SO_4^{2-} ions in

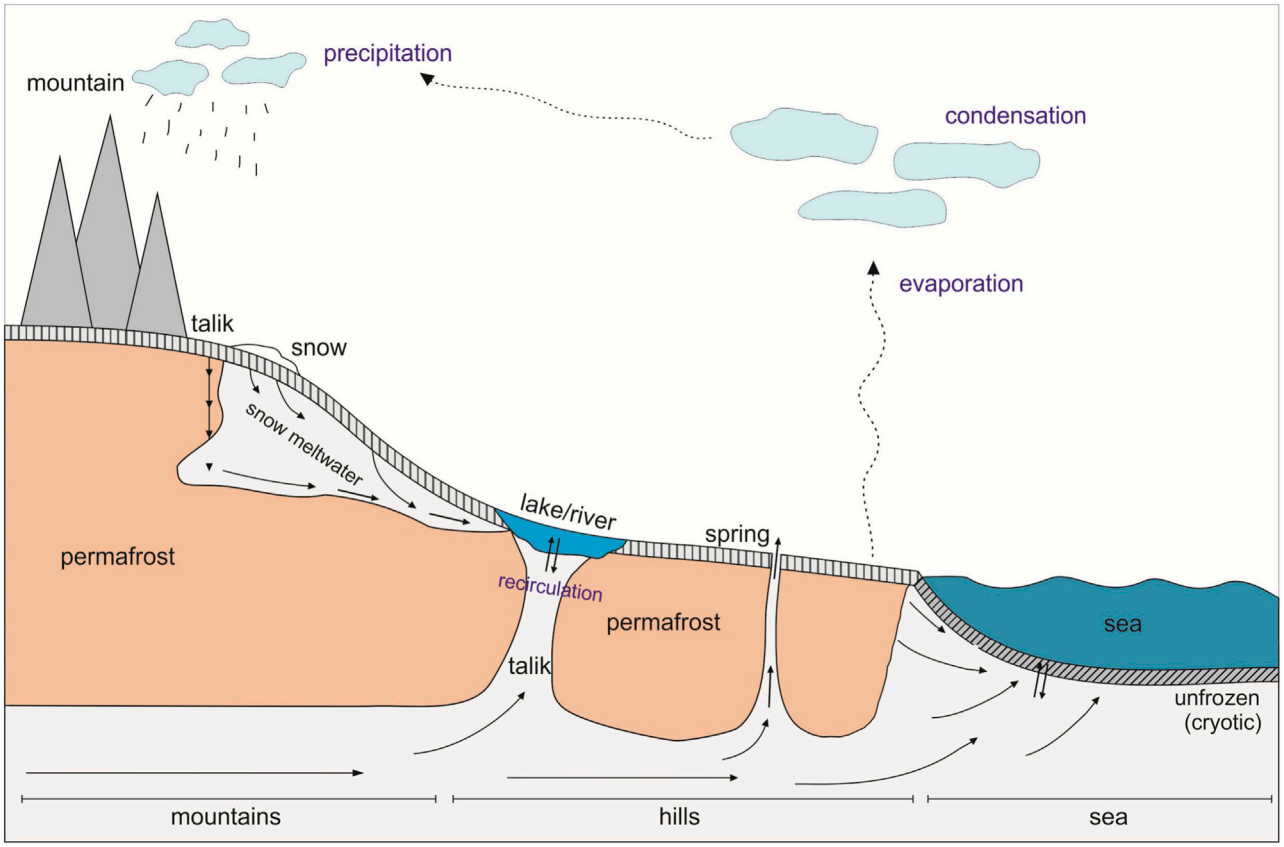

FIGURE 3
Groundwater cycle in the permafrost region. A schematic drawn based on information in Van Everdingen, 1990; Scheidegger, 2013; Ma et al., 2017; Cochand et al., 2019.

Finsterwalderbreen (Spitsbergen, Norway) (Cooper et al., 2002; Lehmann et al., 2023; van Stempvoort et al., 2023). It is worth underling that Cheng and Jin. (2013) found a correlation between recharge/discharge areas and groundwater composition. In recharge areas (mountains), groundwater had lower mineralisation rates than groundwater in discharge areas (basins, valleys, or high plains) (Figure 3) (Cheng and Jin, 2013). In general, the hydrochemistry of suprapermafrost groundwater is characterised by low mineralisation rates and depends on the season and location. The geochemical composition of suprapermafrost groundwater predominantly depends on bedrock lithology and precipitation (Olichwer et al., 2013).

2.2 Subpermafrost groundwater

Unlike groundwater from suprapermafrost zones, subpermafrost groundwater revealed considerably higher values of mineralization. For instance, in the continuous permafrost zone of Siberia, the intrapermafrost groundwater from the Cambrian and Upper Proterozoic aquifer exhibited a high value of mineralization (Alexeev and Alexeeva, 2003). As thermal springs constitute discharge points of subpermafrost groundwaters, extensive research on the chemical composition of spring waters in the Hornsund region (Spitsbergen) was also conducted (Olichwer et al., 2013). The input of precipitation or snowmelt water to thermal springs during the summer season was negligible. The studies showed a diversity in the chemical composition of the thermal waters, indicating various inflows of seawater into the springs. For example, one of the springs was mainly composed of Cl^{-}-Na^{+}, while other one was composed of Cl^{-}–HCO_3^{-}-Na^{+}–Ca^{2+}–Mg^{2+} type. The comparison of chemical properties of thermal waters during the years 1972–2006 revealed a continuous increase in the concentration of all major ions in spring. These changes were attributed to the decline of the ice sheet, which reflects the subsequent progressive decrease in water circulation in the subpermafrost zone (Olichwer et al., 2013). A similar effect of subpermafrost groundwater mixing with seawater was observed in the Buor-Khaya Gulf (Siberian Arctic) (Charkin et al., 2017). This led to the transformation of groundwater into salt water (salinity of 22) (Charkin et al., 2017).

High mineralization was also observed in samples from wells in QTP, where the majority (more than 60%) exceeded 1,000 mg L^{-1} (Table 2) (Cheng and Jin, 2013). The subpermafrost groundwater of QTP in the Triassic aquifer was characterized mainly by the presence of Cl^{-}-Na^{+} (comes from karst or artesian saline groundwater) and Cl^{-}·$HCO_3^{-}$$Na^{+}$·$Ca^{2+}$, and within burial depths the mineralization rate increased (Cheng and Jin, 2013). Groundwater in the Hulugou catchment of QTP indicated a stronger water–rock interaction and weaker evaporation compared to suprapermafrost groundwater. It was hypothesized

that during the warm season, the subpermafrost groundwater could be fed by different sources from the suprapermafrost aquifer, thermokarst pools, glacier and snow meltwater (Ma et al., 2017). Similarly to Arctic regions, studies in the Hulugou catchment showed that mineralization values of subpermafrost groundwater were also higher than those of suprapermafrost groundwater (Hu et al., 2018). The lowest values in the range (Table 2) probably corresponded to the infiltration of suprapermafrost groundwater through sinkholes. The subpermafrost groundwater of the pre-upper Cretaceous Hulugou catchment was classified as HCO_3^-·SO_4^{2-}-Mg^{2+}·Ca^{2+} water and most probably carbonate and gypsum were responsible here for its composition (Table 2) (Hu et al., 2018).

In summary, permafrost has been perceived as the main factor controlling the chemical composition of subpermafrost groundwater in permafrost zones. This groundwater is predominantly recharged and discharged through open taliks. Subpermafrost groundwater is characterized by a long cycle time and low flow rates, and therefore groundwater revealed high mineralization rates. The hydrochemistry of subpermafrost groundwater is spatially variable and has significant vertical discrepancies that are caused by heterogeneity in groundwater dynamics. The presentof lithologic variations and changes in water-rock interactions may be the main factor affecting the subpermafrost groundwater chemistry.

2.3 Intrapermafrost groundwater

The intrapermafrost aquifer is positioned within the taliks, surrounded by permafrost (van Everdingen et al., 1990). Studies conducted in Spitsbergen (Svalbard Archipelago), central Yakutia (eastern Russia), and the Hulugou catchment (northeastern QTP) showed that intrapermafrost groundwater has high mineralization close to subpermafrost groundwater and is dominated by $HCO_3^-$$Ca^{2+}$-$Mg^{2+}$ ions (Olichwer et al., 2013; Pavlova et al., 2016; Ma et al., 2017). Additionally, in Spitsbergen high concentration of SO_4^{2-} ions indicates that this groundwater comes from suprapermafrost groundwater where oxidation of sulphides occurs (Table 2) (Olichwer et al., 2013). Although, the chemical composition of the intrapermafrost groundwater in Spitsbergen can be uncertain because it was determined by hydrochemical analysis of karst spring waters and a thorough analysis was difficult due to the possible mixing of groundwater with seawater (Olichwer et al., 2013). In contrast to the above examples, the groundwater of the intrapermafrost under lakes in Central Yakutia (Siberia) showed that the connection between lakes and groundwater aquifers through the intrapermafrost taliks enables infiltration of surface water and suprapermafrost groundwater with lower salinity into the intrapermafrost (Table 2) (Pavlova et al., 2016). A different situation to the aforementioned cases was noticed in the Hulugou catchment of QTP (Ma et al., 2017). Here, it was deduced the talik was closed and had a negligible hydraulic connection with supra- and sub-permafrost groundwater. Nonetheless, the intrapermafrost groundwater had a long contact time for chemical reactions between water and rock in a closed environment (Ma et al., 2017). Thus, the intrapermafrost groundwater in the Hulugou catchment of QTP had the highest mineralization as well as the high concentration of $HCO_3^-$$Ca^{2+}$-$Mg^{2+}$ ions, which significantly exceeded those observed within suprapermafrost or subpermafrost aquifers in this region (Table 2) (Ma et al., 2017). In summary, the chemical composition of the intrapermafrost groundwater is variable and difficult to estimate because of the implication of many factors such as the possible connection between suprapermafrost and subpermafrost groundwaters, flow path, rock-water interaction, water residence time, and hydrological cycle.

3 Groundwater recharge

Groundwater recharge is the flow of water from the surface to the underground and can be described as residual after subtraction of runoff, evapotranspiration, and accumulation of change in water storage from precipitation (Dhungel et al., 2016). Groundwater recharge and storage are the most difficult components of the water budget to quantify and are affected by the amount and intensity of precipitation, soil and vegetation types, lithology, and topography. Recharge rates in cold region are currently neglected in global estimations, although they may vary in space and time and can be significantly enhanced by climate change (Michel and van Everdingen, 1994; Döll and Fiedler, 2008; Clilverd et al., 2011; Green et al., 2011; Bense et al., 2012). The movement of water in permafrost areas is markedly hindered by ice covers, frozen grounds, glaciers, and snow and groundwater recharge occurs during the warm season (Woo, 2011; Ireson et al., 2013). The highest recharge fluxes are during thaw periods and in some small karstic areas may exceed even 1 $m^3 s^{-1}$ (van Everdingen, 1981; Ireson et al., 2013). In the continuous permafrost zone, or during winter when the active layer is frozen, groundwater recharge is restricted to taliks (Figure 3).

The recharge of intra- or sub-permafrost groundwater is promoted by deep fissures and other passages through karstic rocks such as dolomite, limestone, and gypsum (Woo, 2011). Therefore, net recharge can be positive in regions where precipitation surpasses evapotranspiration (Bhatti et al., 2021). Groundwater recharge can occur during the summer season through organic soils (Utting et al., 2013) e.g., in a mountainous area of Spitsbergen, suprapermafrost groundwater was fed by streams coming from hills and snow melting (Dragon and Marciniak, 2010).

3.1 Recharge by precipitation

In high-latitude regions, a considerable amount of annual precipitation occurs in the form of snow with uneven spatial distribution. It can be percolated into deeper water reservoirs through soils and open systems pingo during the snowmelt season. Moreover, like in nonpermafrost zones, the type of unfrozen soil is also crucial, especially during summer or in discontinuous permafrost regions. Van Everdingen. (1990) claimed that recharge in unfrozen soil occurs predominantly in coarse-grained sediments and less in fine-grained sediments and compact soil. Therefore, in continuous permafrost zones, recharge is mostly restricted to taliks (Clark et al., 2001; Scheidegger et al., 2012; Kane et al., 2013; McKenzie and Voss, 2013; Wellman et al., 2013; Walvoord and Kurylyk, 2016; Crites et al., 2020; Malov, 2021) and in

TABLE 3 Groundwater recharge sources of different aquifers in the continuous and discontinuous permafrost region.

No.	Source/type of the groundwater	Location	Coordinates	Permafrost characterization	References
1	Precipitation	northwestern Canada	62–69°N, 118–140°W	Continuous in the northern flatlands and higher elevations in mountainous regions (55% of study area). Discontinuous permafrost at lower latitudes and elevations (40%)	Crites et al. (2020)
2	Precipitation (Shallow groundwater is young and poorly evolved and is renewed every year mainly by snowmelt infiltration through low-organic soil. Deeper groundwater is also recharged by modern precipitation)	Tasiapik Valley watershed at Umiujaq, Canada	56°33′N, 76°31′W	Discontinuous permafrost zone	Cochand et al. (2020)
3	Glacier Subpermafrost groundwater	Svalbard	74°-81°N 15°-20°E	Continuous zone	Haldorsen et al. (2011)
					Haldorsen et al. (1996)
4	Glacier, precipitation Subpermafrost groundwater	northeastern Alaska	68–70°N, 141–151°W	Continuous zone	Kane et al. (2013)
5	Ice, precipitation in perennial permafrost (in non-glaciated areas) and subglacial waters (in glaciated areas)	Hornsund region, Svalbard	76°57′–77°12′N	Continuous zone	Olichwer et al. (2013)
	Suprapermafrost groundwater				
	Subpermafrost groundwater				
6	Precipitation and infiltration of freshwater from Pechora River	Pechora river valley, western Russian Arctic	67°37′-67°40′W and 52°57′-53°07′N	Continuous zone	Malov (2021)
7	Suprapermafrost groundwater: precipitation	Qaidam Basin, Qinghai Tibetan Plateau	34°40′N and 99°20′E	Discontinuous zone	Bibi et al. (2019)
	Subpermafrost: suprapermafrost groundwater *via* taliks				
8	Precipitation and meltwater: suprapermafrost groundwater	Qinghai Tibetan Plateau	30°–35°N and 90°–95°E	Continuous zone	Cheng and Jin (2013)
	Subpermafrost groundwater: precipitation and suprapermafrost groundwater				

the case of suprapermafrost groundwater to infiltration of the active layer (which can be limited during winter) (Cochand et al., 2020). The research of the continuous permafrost zone in QTP also showed that vertical water penetration was weak and therefore that meteoric water, surface water and shallow groundwater can only laterally or horizontally recharge deep groundwater through taliks or other vertical discontinuities (Bibi et al., 2019). In these regions, meteoric water and melt water are the main sources for recharging the intra- and sub-permafrost groundwater through taliks (Table 3) (Cochand et al., 2020).

Recharge from supra-permafrost to sub-permafrost aquifer is usually low due to low recharge values and long residence time (Haldorsen et al., 2011). In regions with a dry climate and high thickness of the permafrost layer (e.g., the subpermafrost groundwater systems in Svalbard), groundwater recharge is limited (Haldorsen et al., 2010). Furthermore, the study of sub-permafrost groundwater recharge in the eastern North Slope of Alaska showed that recharge from upper layers to the sub-permafrost aquifer was impossible in a permafrost environment due to the presence of ice in soil pores that effectively decreased hydraulic conductivity (Kane et al., 2013). However, the same study showed that higher recharges on the north slope of Alaska were associated with limestone bedrock.

In QTP, groundwater recharge occurs primarily by mountain runoff through infiltration through unconsolidated sedimentary deposits and is associated with geomorphology, landform, fissures, and groundwater reservoirs (Jin et al., 2009; Cheng and Jin, 2013). Cheng and Jin. (2013) showed that the suprapermafrost water in QTP was recharged by meteoric and meltwater through weathered bedrocks and geological fractures. Precipitation and supra-permafrost groundwater constitute the main recharge sources for sub-permafrost groundwater and can be stored in fracture zones along its flow paths. Some of this water can be discharged into depression springs. Another portion of supra-permafrost groundwater infiltrated deeper into the soil and recharged sub-permafrost groundwater through the talik connection, or simply recharged the bedrock fissure water and pore water without an identifiable pathway (Cheng and Jin, 2013). Furthermore, in the northeast QTP, different weather conditions prevail and rainfall dominates, while snowfall is negligible (Pan et al., 2017). Some studies revealed some similar trends in precipitation in Svalbard and the northern part of QTP (Cheng and Jin, 2013). The differences in precipitation between Svalbard and southern QTP can be explained by a poor vapour source that results in less precipitation in southern QTP, while in Svalbard and in the northern QTP, a higher amount of precipitation

was observed. The inner part of the alpine areas of QTP is covered by snow, modern glaciers, and permafrost. The water derived from the melting and precipitation delivers a comparatively high volume of recharged water to this region. Mostly, large steep hills constitute a recharging field for groundwater, while depressions and lowlands serve as groundwater flow and discharge areas (Figure 3).

It should be noted here that also ice-wedge polygons in thermokarst-affected landscapes cause significant changes in snow distribution (Liljedahl et al., 2016). Lowland tundra occupied by low- or high-centred polygons revealed a comparable snow depth at the end of the accumulation season. However, observations conducted in Alaska between 2012 and 2014 showed that low-centred ice-wedge polygons were characterized by almost continuous floods while high-centred ice-wedge polygons by droughts (Liljedahl et al., 2016). Low-centred ice-wedge polygons rims usually accumulate less snow than centers and troughs that lie below the ridges due to wind (Boike et al., 2012; Painter et al., 2016). Moreover, lateral surface/subsurface water flow significantly influences meltwater redistribution during the warm season (Helbig et al., 2012). Complex and highly dynamic ice-wedge polygons landscape strongly control temporally and spatially lateral water fluxes (Helbig et al., 2012).

3.2 Glacially recharged groundwater

In some permafrost areas, such as southern Spitsbergen, glaciers can also contribute to the overall recharged water pool (Olichwer et al., 2013). Glacier meltwater can infiltrate pores or fissures within the bedrock, thus feeding the circulation water network (Haldorsen et al., 2011). Haldorsen et al. (1996) claimed that a small part of the meltwater derived from polythermal glaciers may penetrate the soil and recharge the subpermafrost groundwater system via taliks or other vertical discontinuities.

While in the southern and northern mountainous regions of the QTP characterised by a discontinuous permafrost zone, groundwater recharge and discharge appeared to be, in general, undisturbed (Cheng and Jin, 2013). The suprapermafrost groundwater is mostly fed by meteoric water and glacial meltwater through weathered bedrocks and some fractures or cracks in rocks.

3.3 Recharge through surface water bodies

Groundwater recharge capacities vary spatially, and the importance and significant role of water exchange between surface and groundwater resources via local connections such as taliks was already observed in the 1990s (Scheidegger, 2013). Studies along the reclaimed floodplain in the continuous permafrost area of Yakutia Yakutsk (Russia), showed that the open taliks were an active exchange channel for the Lena River and suprapermafrost groundwater (Pavlova et al., 2020). The exchange mechanism relies on lateral seepage from the Lena River into suprapermafrost groundwater and the magnitude of recharge probably depends on the volume of water in the river (Pavlova et al., 2020). Malov. (2021) observed a similar mechanism and showed that groundwater in the Pechora River (Ural Mountains of northern Siberia) can be recharged by the penetration of meteoric water and infiltration from the Pechora River by the open talik. Studies in the Buor-Khaya Gulf, Laptev Sea) groundwater recharge occurred only through open taliks (Charkin et al., 2017). The authors claimed that one of the main sources of groundwater recharge may be the Lena River water, which can cause the mixing of cryogenic water with fresh surface water. Furthermore, topographic slopes played a crucial role in facilitating water exchange between all depths.

Studies conducted in northeast QTP also revealed that a lake recharged the suprapermafrost aquifer during the dry winter season; however, during wet weather conditions, suprapermafrost recharge decreased significantly and was discharged into the lake (Pan et al., 2017). In the northern Qinghai Lake catchment, groundwater in the piedmont alluvial plain was recharged by lateral seepage of groundwater located in the mountain, while groundwater in the floodplain was recharged by the river (Yao et al., 2015).

In the Arctic and QTP, lakes and rivers can exchange water with groundwater aquifers. Groundwater may be fed by surface water and, depending on the depth of the talik, recharge can connect lakes and rivers with intra- and sub-permafrost groundwater (Table 3) (Woo, 2012).

4 Groundwater discharge

Two types of groundwater discharge can be distinguished: occurring in terrestrial and marine environments. Groundwater discharge into ocean water can proceed through an indirect pathway through surface streams or directly through submarine groundwater discharge (Table 4). Several driving forces might affect SGD, such as tidal pumping, nearshore circulation due to tides and waves, saline circulation driven by dispersive entrainment, brackish discharge, and seasonality (Michael, 2005; Moore, 2010). SGD is described in more detail in Section 4.3, therefore here we focus more on groundwater discharge into the terrestrial zone. Groundwater discharge may supply surface waters such as rivers, lakes and ponds (Figure 3). Furthermore, springs are specific points that are strongly correlated with groundwater discharge (Pollard, 2005; Haldorsen et al., 2010). Terrestrial groundwater flow in permafrost regions is driven by hydraulic gradients (Lamontagne-Hallé et al., 2018). Mathematical evaluation of groundwater discharge on the riverbed and different slopes of the land surface showed that groundwater discharge from the top to the bottom can increase during the winter season as a consequence of the formation of lateral talik (Lamontagne-Hallé et al., 2018). Furthermore, according to simulations based on the conditions of the continuous permafrost environment, the spatial distribution of groundwater discharge into rivers can change markedly as permafrost thaws (Lamontagne-Hallé et al., 2018). Initially, permafrost thaw causes most groundwater to seep directly to the ground surface because of limited linkages between the riverbed and permafrost aquifers. This seepage is uniformly distributed between the upslope and downslope zones (Lamontagne-Hallé et al., 2018). As the temperature increases and the permafrost thaw accelerates, most groundwater seepage is transferred to the river bottom due to increased hydrological connectivity, and therefore the volume of groundwater directed to the upslope decreases significantly. It was estimated that within the next 300 years, the amount of groundwater discharged to the

TABLE 4 Groundwater discharge of groundwater into the marine and terrestrial environment.

No.	Discharge sites/ groundwater type/ dominant driving force	Flux	Location	Coordinates	Permafrost characterization	References
			Terrestrial			
1	Springs (geothermal heat): subpermafrost groundwater Icings (hydraulic pressure): mainly continuous discharge of subpermafrost groundwater, and sometimes intrapermafrost groundwater	Groundwater as a potential source, no data	Axel Heiberg Island, Canada	79° 45′ 0″ N 91° 0′ 0″ W	Continuous permafrost	Pollard (2005)
2	Springs (geothermal heat): subpermafrost groundwater Arctic Ocean: subpermafrost groundwater Icings (hydraulic pressure): subpermafrost groundwater	Groundwater as a potential source, no data	Northeastern Alaska	68° 0′ 0″ N 141° 0′ 0″ W 70° 0′ 0″ N 151° 0′ 0″ W	Continuous permafrost	Kane et al. (2013)
3	Lake (topographically driven flow and permafrost thaw): n.d. (intrapermafrost/ suprapermafrost groundwater)	from 1.6×10^4 m^3 d^{-1} to 2.1×10^4 m^3 d^{-1}	Toolik Lake, (Alaska)	68° 0′ 0″N 149° 0′ 0″ W	From continuous to discontinuous	Dimova et al. (2015)
4	River: suprapermafrost and subpermafrost groundwater	0.6–61.6 mgC L^{-1} HPI: 16%–44%	Yukon River Basin (Canada/Alaska)	61° 0′ 0″ N 141° 0′ 0″ E 68° 0′ 0″ N 151° 0′ 0″ E	Discontinuous (50%–90%) with localized regions of sporadic (10%–50%) and isolated permafrost (<10%)	O'Donnell et al. (2012)
5	Lake (permafrost thaw): subpermafrost groundwater	2000–4,000 m^3 d^{-1} and 2–8 mmol CH_4 m^{-2} d^{-1} (high activity endmember) 4,000–15000 m^3 d^{-1} and 4–16 mmol CH_4 m^{-2} d^{-1} (average endmember)	Yukon Kuskokwim Delta, Alaska	61° 15′ 50.4″ N 163° 14′ 45.6″ W	From continuous to discontinuous permafrost	Dabrowski et al. (2020)
6	Pond (hydraulic gradient): suprapermafrost groundwater	0.1–20 m^3 d^{-1} and 7.6 mmol CH_4 m^{-2} d^{-1}	Stordalen catchment (northern Sweden)	68° 21′ 29.999″ N 18° 58′ 57″ E	Sporadic permafrost	Olid et al. (2021)
7	Ponds (thawing of permafrost): suprapermafrost groundwater	1.2 mmol CH_4 m^{-2} d^{-1}	Stordalen catchment	68° 20′ 59.999″ N 19° 01′ 59.999″ E	Sporadic permafrost	Burke et al. (2019)
8	Ponds: no data	100.6 mmol CO_2 m^{-2} d^{-1} and 10.6 mmol CH_4 m^{-2} d^{-1} (emission from ponds)	Yale Myers Forest, Windham Counties	42° 36′ 0″ N 72° 15′ 0″ E	No data	Holgerson et al. (2015)
9	Glacial meltwater	no data	Spitsbergen	79° 40′ 0″ N 10° 40′ 0″ E	No data	Kies et al. (2011)
10	River (thawing of permafrost)	no data	Yukon River basin (Alaska/Canada)	66° 0′ 0″ N 145° 0′ 0″ W	From continuous permafrost (major part) to discontinuous (minor part)	Walvoord and Kurylyk (2007)

(Continued on following page)

TABLE 4 (*Continued*) Groundwater discharge of groundwater into the marine and terrestrial environment.

No.	Discharge sites/ groundwater type/ dominant driving force	Flux	Location	Coordinates	Permafrost characterization	References
11	Lake	no data	Shellabear Lake (Canada)	74° 49′ 59.999″ N 113° 30′ W	Continuous permafrost	Dugan et al. (2012)
12	Lake (thawing of permafrost): suprapermafrost groundwater	0.5 mmol CH_4 m^{-2} d^{-1} in 2011 0.06 mmol CH_4 m^{-2} d^{-1} in 2012	Toolik Lake, (Alaska)	68° 37′ 59.999″ N 149° 35′ 59.999″ W	Continuous permafrost	Paytan et al. (2015)
			Terrestrial- QTP			
13	River (thawing of permafrost): suprapermafrost	DIC 4.94 mmol L^{-1}, DOC 0.95 mmol L^{-1} (for groundwater samples)	Fenghuo Mountain, TP	34° 45′ 0″ N 92° 52′ 59.999″ E	Continuous permafrost	Song et al. (2020)
14	River and lake (thawing of permafrost): suprapermafrost	3.5 x 10^6 m^3d^{-1} (based on ^{222}Rn calculation)	Lakes and Yellow River, QTP	33° 46′ 04.439″ N 99° 39′ 27.720″ E 34° 36′ 08.989″ N 98° 16′ 13.439″ E	Continuous and discontinuous permafrost and seasonally frozen soil	Yi et al. (2018)
15	Lake	LGD: 7.67 × 10^6 m^3 d^{-1} (radium inventory model) and 8.52 × 106 m^3 d^{-1} (radium eddy diffusion model)	Qinghai Lake, QTP	28° 27′ 21.999″ N 98° 45′ 38.999″ E	No data	Kong et al. (2019)
16	Lake	LGD: 4x10^4± 3x10^4 m^3 d^{-1}; 0.78 mmol m^{-2} d^{-1} and 0.003 mmol m^{-2} d^{-1} for DIN and DIP Riverine nutrients: 1.19 mmol m^{-2} d^{-1} for DIN and 0.053 mmol m^{-2} d^{-1} for DIP	Ximen Co Lake, QTP	33° 23′ 31.599″ N 101° 06′ 12.200″ E	Discontinuous and isolated permafrost	Luo et al. (2018)
17	Lake (precipitation and active layer thaw) Suprapermafrost	11 m^3 d^{-1}—43 m^3 d^{-1} during three ice-free seasons	QTP	36° 49′59.999″N 102° 30′0″E	Discontinuous permafrost	Pan et al. (2017)
			Marine			
1	Sea (pressure gradient): subpermafrost groundwater	Buor-Khaya Gulf discharge *via* tectonogenic talik equal to 1.7 x 10^6 m^3 d^{-1} Lena River 123 x 10^6 m^3 d^{-1} Yana River (in April) 0.06 x10^6 m^3 d^{-1}	Buor-Khaya Gulf, Lapatev Sea	72° 0′0″N 130° 0′0″E	Continuous subsea	Charkin et al. (2017)
2	Sea (thawing of permafrost): submarine permafrost	Scenario: SO_4^{2-} —2.4 m^2d^{-1}, CH_4-4.5 m^2d^{-1}	Chukchi Sea	73° 37′13.302″N 166° 25′43.974″W	Subsea permafrost	Kim et al. (2021)
3	Kasitsna Bay (tidal pumping): subsea permafrost Point Barrow (permafrost thaw): subsea permafrost	av specific discharge 1.9 m day^{-1} (Kasitsna Bay); av specific discharge 0.01 m day^{-1} (Point Barrow)	Kasitsna Bay, Point Barrow (Alaska)	59° 0′0″N 151° 0′0″E 71° 0′0″N 156° 0′0″W	Sporadic (Kasitsna Bay), continuous (Point Barrow)	Dimova et al. (2015)

(Continued on following page)

TABLE 4 (*Continued*) Groundwater discharge of groundwater into the marine and terrestrial environment.

No.	Discharge sites/ groundwater type/ dominant driving force	Flux	Location	Coordinates	Permafrost characterization	References
5	Sea coast (terrestrial<10%, topographic gradients): suprapermafrost	8.6×10^3 to 4.2×10^4 m^3 d^{-1}, 23–118 × 10^6 mmol DOC d^{-1}, 1.21–6.14 × 10^6 mmol DON d^{-1}	Eastern Beaufort Sea coast (Alaska)	70° 02′0″N 143° 10′0″W 70° 07′0″N 144° 10′0″W	Continuous permafrost	Connoly et al. (2020)
6	Ocean (tidal pumping, hydraulic gradient- Kasitsna Bay, low tidal pumping, low hydraulic gradient- Elson Lagoon and the Beaufort Sea): subsea permafrost	Kasitsna Bay (120 m^3 d^{-1} m^{-1} of shoreline) NO_3^- 3.86 × 10^{10} mmol d^{-1}	Kasitsna Bay	70° 0′0″N	Sporadic permafrost (Kasitsna Bay)	Lecher et al., 2016a; Lecher et al., 2016b
		SiO_4^{4-}1.20 × 10^{11} mmol d^{-1}, 4.3 × 10^3 NO_3^- mmol d^{-1} m of shoreline^{-1}, 13 × 10^3 SiO_4^{4-} mol d^{-1} m of shoreline^{-1}	Elson Lagoon, Beaufort Sea	160° 0′0″W	Continuous (Elson Lagoon)	
		Elson Lagoon (12 m^3 m^{-1} d^{-1}; 0.74 mmol CH_4 m^{-1} d^{-1}), NO_3 0.50 mol d^{-1} m of shoreline^{-1}, 0.3 × 10^3 SiO_4^{4-} mmol d^{-1} m of shoreline-1	Cook Inlet	60° 0′0″N		
		Beaufort Sea 1.20 × 10^3 NO_3^- mol d^{-1} m of shoreline^{-1}, 0.52 × 10^3 SiO_4^{4-} mmol d^{-1} m of shoreline^{-1}, CH_4 0.26 mmol m^{-1} d^{-1}	Gulf of Alaska	150° 0′0″W		
		Cook Inlet				
		SiO_4^{4-}7.77 10^9 mmol d^{-1}				
		NO_3^- 2.50 10^9 mmol d^{-1}				
		Gulf of Alaska River contribution				
		SiO_4^{4-}1.14 10^{10} mmol d^{-1}				
		NO_3^- 2.16 10^9 mmol d^{-1}				
7	Fresh SGD to ocean: no data	Sea CH_4 3.5–30.0 10^{-3} mmol/ cm^2/yr (Lofoten-Vesterålen, Norwegian Sea)	Hornsund fjord (Spitsbergen) Storfjordrenna gas hydrate mounds (Spitsbergen), Lofoten-Vesterålen	68° 09′30.200″N 010° 27′35.600″E 76° 06′24.800″N 015° 58′03.699″E 76° 58′59.900″N 016° 16′09.500″E 76° 58′37.200″N 015° 50′58.599″E	Sporadic/isolated permafrost	Hong et al. (2019)
8	Fresh SGD to sea: no data	no data	Beaufort Sea	71° 19′03.399″N 143° 59′53.499″W 71° 19′02.600″N 143° 59′58.899″W	Subsea permafrost	Hart et al. (2011)
9	Fresh SGD to sea: no data	no data	Beaufort Sea	70° 47′25.162″N 135° 33′38.336″W	Subsea permafrost	Paull et al. (2015), Paull et al. (2022)

(Continued on following page)

TABLE 4 (*Continued*) **Groundwater discharge of groundwater into the marine and terrestrial environment.**

No.	Discharge sites/ groundwater type/ dominant driving force	Flux	Location	Coordinates	Permafrost characterization	References
10	Fresh SGD to sea: no data	no data	Kara Sea	72° 58′17.400″N 068° 53′40.300″E	Subsea permafrost	Semenov et al. (2019)
11	Fresh SGD to sea: no data	$3.1x10^4$ m^3d^{-1}	Greenland shelf	65° 02′50.399″N 039° 17′29.500″W	Subsea permafrost	DeFoor et al. (2011)
12	Fresh SGD to sea: no data	$0.012x10^6$ m^3d^{-1}	Cambridge Fiord, Baffin Island	72° 57′10.599″N 074° 33′00.200″W	No data	Hay et al. (1984)
13	Fresh SGD to sea (permafrost thaw): subsea permafrost	no data, 90% of the maximum freshening ratio	Svalbard fjords	78° 24′48.156″N 017° 06′29.465″E	Subsea permafrost	Kim et al. (2022)

upslope (e.g., wetlands) decreases by approximately 50%, while the amount of groundwater flowing to the river bottom increases 15 times compared to the current state (Lamontagne-Hallé et al., 2018). This can be caused by a possible lowering of the permafrost table. Other studies also confirmed similar future expectations for increased groundwater discharge to surface water (Ge et al., 2011; Bense et al., 2012; Frampton et al., 2013; Evans and Ge, 2017; Evans et al., 2018).

4.1 Groundwater discharge to rivers, lakes, and ponds

Solute transport through groundwater flow can pose a potential threat to the environment, especially in permafrost thaw regions, where newly released groundwater can contain increased amounts of chemicals such as nutrients, heavy metals, persistent organic pollutants, and greenhouse gases (Hong et al., 2019). Here, we present the characteristics and variability of OM, DOM, and CH_4 associated with groundwater discharge (Table 4).

The significance of the contribution of groundwater to the overall DOM (Table 4) depends on the hydrogeological and geological conditions of the surrounding environment. DOM can be adsorbed on mineral surfaces and/or mineralized under appropriate conditions such as the availability of suitable catalysts, the presence of oxygen, transition metals and/or sunlight (Kleber et al., 2021). Studies carried out in the Yukon River Basin located in Alaska investigating seasonal changes in the chemical composition of DOM in groundwater and used a simplified mixing model to predict future changes in DOM composition and concentration with increased groundwater flow into the river in the area covered in 50%–90% by discontinuous permafrost (O'Donnell et al., 2012). Data obtained for summer-autumn and winter were differentiated and, for example, during the cold season, the discharge was characterised by low DOC concentration (lower than 0.17 mmol L^{-1}), low aromatic content of DOM, and high content of hydrophilic organic matter (HPI) fraction. Based on these calculations, it was suggested that improved permafrost thawing and groundwater discharge will lead to an increase in HPI proportion and a reduced concentration of DOC and higher aromaticity of DOM during summer flow (O'Donnell et al., 2012).

Groundwater can also be a substantial source of CH_4 in lakes (Paytan et al., 2015; Dabrowski et al., 2020). Controls of methane fluxes in permafrost regions through groundwater discharge are complex and depend on environmental conditions that can allow efficient transport of methane into surface waters such as high methane content in the active layer, and the presence of minerotrophic wetlands. Dabrowski et al. (2020) observed that groundwater flows in Landing Lake and Toolik Lake were comparable, although it was shown that the CH_4 input flux was one order of magnitude higher in Landing Lake than in Toolik Lake (Table 4). These differences were due to an almost 18-fold higher concentration of CH_4 in groundwater discharged into Landing Lake than into Toolik Lake, which in turn was explained by the shallow active layer and the small amount of OM in the active layer in Toolik Lake (Dimova et al., 2015). The estimated contribution of groundwater to subarctic ponds located in the sporadic permafrost zone of the Stordalen catchment (subarctic region of northern Sweden) ranged from 6% to 46% of the volume of the pond per day (Olid et al., 2021). The thawed subarctic ponds were supersaturated with CH_4. The contributions of CH_4 from the active layer to the thawed pond were found to be higher than those observed in Alaskan lakes (Olid et al., 2021). The reason for this phenomenon was the higher groundwater flux to the studied ponds than to the Alaskan lakes. CH_4 flux varied between the examined ponds and periods, reaching the highest value in July (Olid et al., 2021). However, based on the estimation of total emissions derived from small ponds with surface area <0.001 km^2 in the permafrost region of the Northern Highland Lake District (northern Wisconsin, United States) north of 50° N, it was deduced that ponds are a main source of CH_4 emission at high latitudes. CH_4 from ponds constituted 40% of global diffusive CH_4 emissions (Holgerson, 2015). Moreover, Christensen and Cox. (1995) presented CH_4 fluxes in the Stordalen with values exceeding those obtained by Olid et al. (2021) by more than twice

depending on the subhabitat types. The highest CH_4 fluxes were recorded under minerotrophic conditions and also indicated that disturbed habitats and, consequently, vegetation composition may entail projected changes in CH_4 emissions. The estimated change in CH_4 flux between 1970 and 2000 revealed that CH_4 emissions could increase by up to 2.1×10^5 mmol of CH_4 per day in the case of wet precipitation. Progressive loss of permafrost in subarctic Alaska and Canada has been observed to cause the rise of wetlands (Jorgenson et al., 2001). However, Oechel et al. (2000) described the opposite effect in the continuous permafrost region of northern Alaska. Furthermore, studies of 52 ponds in the Stordalen Mire and Storflaket bog (east of Abisko, northern Sweden) carried out by Kuhn et al. (2018) showed that the CH_4 fluxes between the ponds did not differ significantly. However, they compared results from various ponds based on the classification of dominant vegetation and hydrologic status, while Burke et al. (2019) classified ponds into four types by taking into account statistical divergences in daily CH_4 flux and discovered that these variations appeared to overlap with the ponds' apparent physical differences, for instance, relative depth, vegetation type, and hydrologic status.

Luo et al. (2018) emphasised the importance of groundwater discharge as a significant pathway for DIN delivery into Ximen Co Lake (Nianbaoyeze MT, eastern margin of the QTP) comparable to those obtained by river runoff. It was revealed that in isolated and discontinuous permafrost regions, groundwater discharge to the Lake Ximen Co. was the second main source of DIN with a contribution of 43%. On the contrary, DIP flow through groundwater only 6.3% of the total DIP load to the lake (Luo et al., 2018).

In the continuous permafrost zone of the QTP (Fenghuo Mountain), DOC concentrations in stream water were significantly lower compared to Arctic streams, while DIC concentrations were higher (Song et al., 2019). The authors observed that as the depth of thaw increased during the warm season, the concentrations of DIC and DOC decreased. Furthermore, the SOC densities recorded in the QTP alpine meadows were 3.6–7.7 times lower than those observed in the Arctic and may be the reason for the low concentration of DOC in the QTP catchments. Wang et al. (2017) indicated that groundwater discharge can be responsible for more than 3/4 of total river runoff during the thawing season (studies in Fenghuoshan in central QTP), and therefore higher concentrations of DOC and DIC can be observed in stream water. Frey et al. (2007) also highlighted the importance of the permafrost thaw process, which may reinforce the contribution of groundwater to the carbon cycle of surface waters in this region. In general, the ages of DOC and DIC were older in streams where warmer permafrost and higher groundwater flow were observed. Song et al. (2020) compared the Yangtze River with the Kolyma River and indicated that the unique summer monsoon across the QTP allowed the fluxes of more depleted dissolved carbon isotopes than the Kolyma River. These findings imply that carbon was immediately released through hydrological connectivity and the superior contribution of subpermafrost groundwater.

Recent studies also highlight the importance of microtopography in groundwater discharge (Liljedahl et al., 2016; Harp et al., 2020; Nitzbon et al., 2020; Painter et al., 2023). Harp et al. (2020) described a new three dimensional mathematical model that demonstrated the impact of ice-wedge polygons on seeping of suprapermafrost groundwater into the surface. This water can potentially carry a significant concentration of DOC and nutrients into surface water. The results of the simulations showed that geometric features have a strong effect on the seepage of groundwater. Studies of Harp et al. (2020) focused on inundated low-centred polygons, and, as the authors stated, the noninundated low-centred and high-centred polygons may have different drainage mechanisms. Furthermore, Harp et al. (2020) also revealed that polygon aspect ratios (width to thawed depth) and hydraulic conductivity anisotropy (conductivities in different directions, i.e., vertical to horizontal) influence strongly on drainage pathways and temporal decline of water volume from ice-edge polygon centres. Based on the calculations conducted by Harp et al. (2020), it was concluded that decrease of the aspect ratio (thawed depth becomes deeper with respect to polygon width) causes increase in polygon volume accessibility for the drainage. It was shown that drainage through the active layer occurs largely along the ring-shaped area of the polygon centre near the rims. This drainage mechanism contributes significantly to the direction of the flow of nutrients and advective heat transport toward the head of ice-edge polygons. A comparison of polygons characterised by similar thaw depths but different widths revealed that the drainage of narrower polygons will be more distributed, whereas wider polygons will show more focused drainage. The drainage pathway is the most dispersed in the case of polygons with high aspect ratios and high hydraulic conductivity anisotropy, whereas for ice-wedge polygons with high aspect ratio and low anisotropy, the drainage occurs slower and mostly near their ridges. The rate of water seepage is highest for polygons with low aspect ratios and large anisotropy. Polygon aspect ratio and hydraulic conductivity anisotropy contribute in a similar way to the drainage process. Higher horizontal conductivity relative to vertical conductivity (high anisotropy) allows for the drainage of a larger polygon volume. Therefore, the ice-wedge polygon can be perceived as the fundamental hydrologic landscape unit responsible for terrestrial water flow and discharge and under appropriate conditions (anisotropic polygons with low aspect ratios) water seepage will occur more rapidly and transport of nutrients, the release of methane will be more significant than in polygons with isotropic hydraulic conductivity and high aspect ratios (Harp et al., 2020).

In summary, in both considered regions (Arctic and QTP) a large amount of DOC and DIC is transported through groundwater into surface water. The chemical composition of the groundwater transported depends on the source of the aquifer, whether it comes from the suprapermafrost or subpermafrost aquifer and the condition of the permafrost. Therefore, in discontinuous and continuous permafrost zones, different volumes of various substances can be transported by groundwater. In addition, even in the continuous permafrost region, significant groundwater fluxes can be observed during the thawing cycle. In QTP groundwater fluxes can be two orders of magnitude higher than in the Arctic (Table 4) (Dimova et al., 2015; Yi et al., 2018; Kong et al., 2019).

Furthermore, groundwater could contribute to the exacerbation of greenhouse warming through the transport of released CH_4 (Holgerson, 2015; Olid et al., 2021). The concentration of released CH_4 depends on groundwater flux, CH_4 abundance in the active layer, and subhabitat types (Holgerson, 2015; Dabrowski

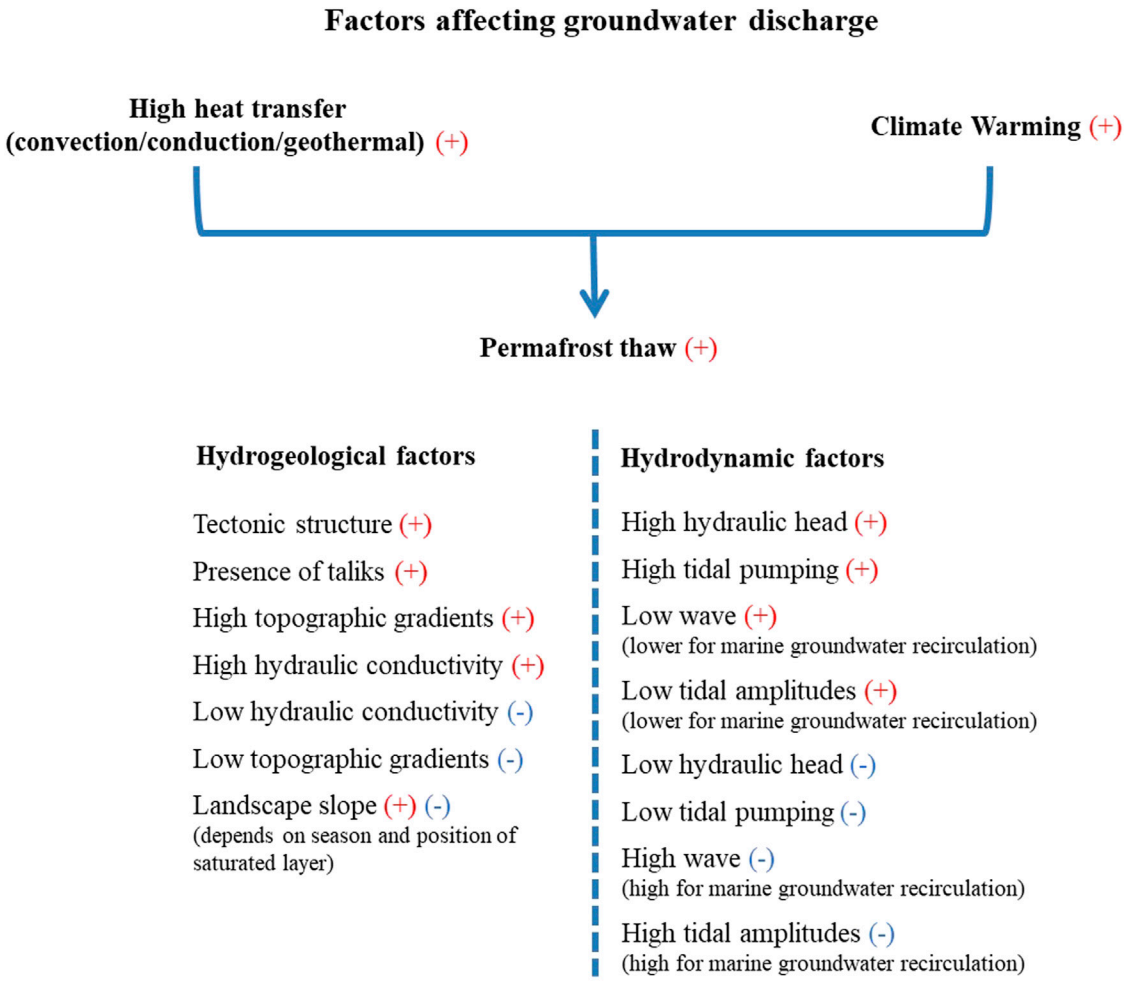

FIGURE 4
Factors influencing groundwater discharge in the permafrost region.

et al., 2020; Olid et al., 2021). In addition, ponds can constitute a significant source of CH4 emission (Holgerson, 2015).

4.2 Groundwater discharge through springs

Springs are common sites mostly related to subpermafrost groundwater discharge (Williams, 1970; Haldorsen et al., 1996; Andersen et al., 2002; Woo, 2011; Grasby et al., 2012). In Svalbard, groundwater discharge occurs primarily through springs (Pollard, 2005; Haldorsen et al., 2010) and particularly from karstic aquifers (Table 4) (Mohammed et al., 2021). Furthermore, the appearance of springs as evidence of active groundwater flow was also recorded in continuous permafrost in northeastern Alaska (Kane et al., 2013). However, the exact source and flow path to these springs remains unspecified. Groundwater discharge through springs is sometimes related to open system pingos, and pingos growth can occur when the maximum discharge rate is up to 3 L s^{-1} and when the groundwater temperature does not exceed 1.2°C (Yoshikawa, 1998). During winter, as freezing starts, groundwater discharge causes a rise of the hydraulic potential in the active layer and the formation of icing blisters (Pollard and French, 1984). Springs can serve as sites for continuous sub-permafrost groundwater discharge throughout the year. Washburn (1969) recorded continuous groundwater discharge at a pressure of 170 kPa. Temperatures at different spring outflows can be almost unchanged throughout the year (Pollard, 1991; Pollard et al., 1999; Omelon et al., 2001; Andersen et al., 2002). In addition, a 55-year study on Axel Heiberg Island in the Canadian high Arctic showed that the average discharge temperature of the individual springs differed by less than 0.5°C (Pollard et al., 1999). Pollard et al. (1999) reported that the groundwater discharge rate for springs can vary significantly from almost imperceptible to 1.5 L s^{-1}. Although the groundwater discharge rate of individual springs was low (<0.5–2.0 L s^{-1}), the total discharge of 20–40 springs can be more pronounced and reach combined discharge rates in the range of 10–15 L s^{-1}. Furthermore, studies in Adventdalen (Isfjorden, Svalbard) showed that four of six open system pingos were active

places for groundwater discharge throughout the year and can play a significant role as potential hot spots for greenhouse gas emissions (Hodson et al., 2019; Hodson et al., 2020). The discharging subpermafrost groundwater in Svalbard pingos were brackish, with a mostly low concentration of oxygen, nitrate and sulphate suggesting the occurrence of microbially mediated transformations (Hodson et al., 2020). In alpine regions of QTP, springs and pingos are also associated with subpermafrost groundwater discharge (Cheng and Jin, 2013). However, part of the suprapermafrost groundwater in the discontinuous permafrost zone recharged by meteoric water may overflow onto the ground surface as depression springs (Cheng and Jin, 2013). The QTP is specific because it is mainly characterised by the appearance of thermal springs (more than 300 springs have been identified in the permafrost zone) with a temperature range of 40°C–72°C andenriched in rare chemical elements (Cheng and Jin, 2013). The highest detected groundwater discharge rate in QTP was 8.3 L s^{-1} and was 4–16 times higher than that measured in individual springs in Svalbard (Pollard et al., 1999; Cheng and Jin, 2013). In basins located between mountains in the continuous permafrost zone, the relatively stable permafrost layer creates a low-permeability underground layer that inhibits groundwater flow. However, in areas where thermal springs are present, permafrost growth is highly limited.

4.3 Submarine groundwater discharge

SGD is defined as the flow of water through continental and insular margins from the seabed to the coastal ocean, regardless of the composition of the fluid or the driving force (Figure 4) (Burnett et al., 2003; Church, 1996; Taniguchi et al., 2019). Therefore, SGD is a sum of two components: net submarine groundwater discharge (freshwater component) and recirculated saline water discharge (marine component). The second component is composed of recirculated seawater due to wave and tidally driven oscillations and convection. According to global estimation, groundwater discharge into the oceans is responsible for 1%–10% of all freshwater inflow into coastal water. The rivers account for the remainder (90%–99%) (Church, 1996; Burnett et al., 2003; Moore, 2010; Luijendijk et al., 2020). However, mobilisation and subterrestrial release of organic and inorganic matter through groundwater discharge are in many regions higher compared to river runoff even by several orders of magnitude (Church, 1996; Swarzenski et al., 2001; Slomp and Van Cappellen, 2004; Santos et al., 2021). On regional and local scales, groundwater discharge can substantially affect coastal biogeochemistry (Szymczycha et al., 2020; Moosdorf et al., 2021; Böttcher et al., 2023).

According to Charkin et al. (2017), SGD in the polar regions depends on the thermal state of the permafrost and the morphological characteristics of the shelf (Table 4). Geological factors such as conducive lithological characteristics (for example, the presence of some fractures in the rock and permeable material), and the formation of channels that combine subpermafrost groundwater with the marine water column are the factors that facilitate SGD. Fresh groundwater flow produces approximately 1%–10% of total groundwater discharge in the coastal system (Burnett et al., 2003; Dimova et al., 2015). However, under appropriate conditions, such as strong hydraulic head gradients, low wave, and lower input of recirculated saline SGD, this contribution may be higher or even 30%. Connolly et al. (2020) estimated that in the case of the Kaktovik Lagoon suprapermafrost, groundwater discharge originating from a terrestrial source was lower than 10% due to flat topography, low amplitudes of tides and waves, and the presence of continuous permafrost. Lecher et al. (Lecher et al., 2016a; Lecher et al., 2016b) also emphasised the importance of ocean forces on SGD fluxes to the coastal Beaufort Sea, on the coast of Elson Lagoon (Arctic Ocean coast of Alaska near Point Barrow) and Kasitsna Bay (Southern Coast of Alaska). Observations in 2011 (August) and 2012 (July) along Kasitsna Bay indicated that groundwater discharge values were comparable during this period as a result of similar tidal amplitudes over the years. SGD in the Arctic can be a source of chemicals such as CH_4, DOC, DON, nutrient, etc.

It has been recognised that SGD can be an important conduit for the transport of methane, the second most important greenhouse gas with a significantly higher warming potential than CO_2. Enormous amounts of methane are stored in the Arctic and can be released into the atmosphere as permafrost thaws (Shakhova et al., 2014). However, CH_4 migration pathways into the oceanic water column are complex and existing data still contain many uncertainties and numerous deficiencies. The latest estimates of methane hydrates in Arctic regions showed that 20 and 45 Pg C are buried in the permafrost and subsea permafrost, respectively (MacDonald, 1990; Ruppel, 2015). The discharge of submarine groundwater in the continuous permafrost zone is rather restricted to the seasonal period of thawing of the permafrost. Dimova et al. (2015) claimed that in the winter season, most of the underground in the Arctic is frozen, and groundwater movement is reduced or inhibited. However, studies also confirmed that groundwater flow rates in the region covered with discontinuous permafrost differ significantly during seasonal freezing and thawing processes in the upper layer (Liao, 2018). In Alaska territory occupied by discontinuous permafrost zones, average horizontal flow rates in winter were one order of magnitude lower than in summer. As a consequence, groundwater movements were low and limited to permafrost-free zones.

Research conducted during the late summer in the continuous permafrost zone showed that total groundwater discharge to the Kaktovik lagoon (Alaska, United States) (Connolly et al., 2020) is a significant source of DOC compared to other sources (Alaska, United States) (Dimova et al., 2015). DOM concentrations obtained in adjacent rivers were 100 times lower than those for suprapermafrost groundwater, and therefore the contribution of groundwater to the transport of terrestrial DOM to coastal water was much more notable and may reach 14%–70% of total DOC and 15%–72% of total DON transported to the north slope of the Alaska Beaufort Sea (Table 4).

Higher groundwater discharge fluxes in Kasitsna Bay also mean higher methane flux from the active layer of thawing (Lecher et al., 2016a; Lecher et al., 2016b). The methane flux into the Elson Lagoon was nearly three times higher than in the Beaufort Sea, although these sites had similar SGD flux. The main reason for this discrepancy was the three times higher CH_4 concentration of coastal groundwater in Elson Lagoon than in the Beaufort Sea. Furthermore, SGD volume fluxes may differ significantly depending

on the method used, i.e., radon- and radium-based discharge. For example, the results of the radium-based flux for Kasitsna Bay and Elson Lagoon were approximately ten times lower than those received from the calculation of radon-based groundwater fluxes. However, for the Beaufort Sea, both measurements were consistent and exhibited almost the same values. A reasonable explanation was the considerable amount of fresh groundwater that was dripping into the Elson lagoon from the active layer without contact with saline water. Therefore, in contrast to radium-based methods, higher values were obtained when the estimation was based on radon methods, as this approach includes brackish, saline, and fresh groundwater, whereas the latter is omitted in the case of radium. Furthermore, radon-based estimations involved river discharge in the SGD flux, while radium-based discharge discards river contribution, leading to lower SGD volume fluxes (Lecher et al., 2016a; Lecher et al., 2016b).

The high concentrations of NO_3^- and SiO_4^{4-} present in groundwater suggest that SGD appears to be a substantial source of nutrients for Kasitsna Bay. Taking into account the average concentration of nutrients in groundwater, the SGD flux and the length of the runoff from the coastline, the river into Kasitsna Bay transported approximately 17.5 and 8.4 times less NO_3^- and SiO_4^{4-}, respectively (Table 4). Measurements in Cook Inlet with a similar tidal oscillation and soil structure to Kasitsna Bay showed that SiO_4^{4-} fluxes delivered by SGD were roughly ten times lower than those supplied by river flux to the entire Gulf of Alaska, while NO_3^- flux revealed a similar contribution as rivers to the Gulf of Alaska. Observation of NO_3^- and PO_4^{3-} in the Beaufort Sea and Elson Lagoon revealed an increase in concentrations near the coast and in coastal groundwater, which indicated that SGD is an important source of nutrients for the Beaufort Sea. Nutrient fluxes for the Beaufort Sea and Elson Lagoon were markedly lower than those demonstrated in Kasitsna Bay. High SGD-derived nutrient fluxes were ensured by large 8 m tides, which appeared to maintain similar SGD magnitude throughout the year. In addition, SGD could be an important source of trace metals for the Arctic Ocean. As permafrost thaws, the amount of nutrients released can increase dramatically due to increased SGD flow (Lecher et al., 2016a).

In the continuous subsea permafrost region of Siberia, the tectonic structure of the shelf had a significant impact on the SGD and the most advantageous conditions for the discharge of pressurised subpermafrost groundwater were created in the rifting of active fault zones (Figure 4) (Charkin et al., 2017). The mechanism of groundwater discharge at fault crossings relied on the upward movement of groundwater due to the expansion of the crushing process of rocks, and also the thawing of the permafrost increased as an effect of a higher geothermal heat flux. Here, SGD in the Buor-Khaya Gulf (Laptev Sea, Siberian Arctic) was marginal compared to the Lena River discharge in April, but for the Yana River discharge in April, the value was more than ten times lower than that of SGD. However, the estimation of SGD was done only for a small part of the Buor-Khaya Gulf, and if considering the entire east Siberian Arctic Shelf zone, the magnitude of SGD must be significantly higher (at least ten times higher, Charkin et al., 2017). Furthermore, the pressurised groundwater discharge mechanism had a more significant contribution than that based on hydraulic forces triggered by newly frozen sediments (Charkin et al., 2017).

In summary, SGD can be a substantial source of DOC and nutrients that could even exceed the loads transported by river runoff. What is more, dissociation of methane hydrates in the Arctic may occur, and SGD may act as methane conduits. Therefore, more attention should be paid to identifying sites of possible gas hydrate destabilisation, as the threat of the release of greenhouse gas into the atmosphere is increasing with global warming. Still, systematic studies in different regions are needed to obtain a complete overview of the situation.

5 Discussion: impact of climate change on groundwater discharge

Before 2010, heat conduction was the only factor that has been taken into account in most simulations of permafrost dynamics and prediction of permafrost degradation. However, numerous studies have shown that groundwater flow and advective heat transfer through an aquifer system should be perceived as one of the most contributing factors that influence permafrost dynamics (Dagenais et al., 2020). Heat conduction is strictly correlated with the temperature gradient, which increases at the surface when the geothermal gradient increases. However, heat advection is defined as heat exchange through groundwater flow or in unsaturated soil through air movement. Generally, Wellman et al. (2013) noted that groundwater advective heat transfer can contribute to permafrost degradation. The distribution of permafrost in a lake's watershed depends on the exchange of groundwater with the lake through suprapermafrost and sublake taliks, but also permafrost influences groundwater flow. The results of simulations supported by field surveys in Umiujaq, Canada, covered by discontinuous permafrost, suggested that groundwater flow could increase the temperature of the subpermafrost aquifer (Dagenais et al., 2020). Furthermore, the permafrost is thinner if heat transfer occurred through a combination of advection-conduction (Dagenais et al., 2020; Jamin et al., 2020). Rowland et al. (2011) also found that subpermafrost groundwater contributes to a reduction of permafrost thickness and talik formation which accelerates permafrost degradation. Their results showed that the thicknesses of the permafrost were five and two times lower with the presence of groundwater flow 20 and 50 m below the ground surface, respectively. Wellman et al. (2013) speculated that subpermafrost groundwater flow may have a comparable force that affects talik development as climatic factors. The intensity of the advective heat flow rate is highly dependent on the magnitude of groundwater flow, which is dependent on aquifer-specific storage and permeability (Scheidegger, 2013). These agree with later studies by Ghias et al. (2017), which found that permafrost thawing can be propelled by both conductive heat transfer and thermal advection originating from groundwater flow during seasonal freeze-thaw cycles; however, the contribution of thermal advection is limited to permeability soil, which can significantly reduce the importance of advection. Moreover, recent calculations showed that the omission of advective heat transport can provide an error lower than 5% (Gao and Coon, 2022). According to Gao and Coon, (2022), it is incomparably more important to consider soil cryosuction which can cause 50%–60% error in discharge.

However, in the discontinuous and sporadic permafrost region in the subarctic territory of Sweden, groundwater heat advection may play an essential role in heat transfer within taliks and possess

the potential to alter the freeze-thaw process (Sjöberg et al., 2016). Chen et al. (2020) pointed out the relationship between groundwater and permafrost in conjunction with the water enrichment of soil groundwater motion. In the area composed of aquitards, groundwater had little or no impact on permafrost. Permafrost is thermally stable and bulky in groundwater-deficient territory. The opposite features are presented by the region rich in groundwater, in this environment the permafrost equilibrium is being upset.

Furthermore, understanding energy and water transport in conjunction with fusion enthalpy can significantly facilitate understanding of the mutual interaction between permafrost thaw and groundwater flow (Bense et al., 2009; McKenzie and Voss, 2013; Ghias et al., 2017; Lamontagne-Hallé et al., 2018). The thawing and freezing processes are associated with the enthalpy of fusion release or absorption, respectively. Loss of enthalpy of fusion can contribute to a reduction in permafrost thaw. For example, McKenzie and Voss. (2013) deduced that advectively triggered permafrost thaw can occur slower in discharge regions, as the down flowing warm recharge water is cooling due to loss of enthalpy of fusion. The most intense advection-influenced permafrost thaw occurs below the hilltops.

Based on the scenarios prepared by Guimond et al. (2022)scenarios between 1980 and 2100 will be observed in the future and it depends on the warming rate and sea level. The first scenario with a high warming rate and low sea level change revealed that coastal groundwater discharge will increase by up to 58% by 2100. However, the second scenario with a high warming rate and a higher rise in sea level showed a lower increase of groundwater discharge equal to 21% due to a decrease in land-sea hydraulic gradients. According to the calculation, the lowest increase in groundwater discharges up to 8% can be predicted under lower warming and low sea level rise (Guimond et al., 2022). In addition, degradation of the geomorphological features of the polygonal tundra can strongly influence water balance due to the formation of troughs and the position of the ice edge centre higher than the rims (Liljedahl et al., 2016). This change will cause an alteration in snow distribution and as a result it will increase runoff and decrease inundation of ice-wedge centers (Liljedahl et al., 2016). Furthermore, simulations conducted by Nitzbon et al. (2020) showed that the thermokarst process can significantly accelerate permafrost degradation even within a few years. Nevertheless, the latest research finding on topographic influence on permafrost degradation showed different conclusions (Painter et al., 2023). It was deduced that potential abrupt acceleration of permafrost degradation due to thaw subsidence is unlikely, because of formation of drier tundra conditions. However, the global impact of thermokarst on permafrost degradation in the upcoming decades is unknown. Simulation under the high global warming scenario indicated a more significant transition of low-centred to high-centred ice-wedges and ultimately formation of larger thermokarst lakes (Nitzbon et al., 2020).

In summary, progress in climate warming is likely to accelerate permafrost degradation, which improves hydrological connectivity due to increased sub-permafrost groundwater flow through talik channels and higher suprapermafrost groundwater flow. The type of soil is of great importance in the flow of groundwater and permafrost dynamics. Differentiated soil permeability and various geological mixtures significantly alter the path and flux of groundwater flow and can also influence the formation of permafrost. Advective heat transfer through groundwater flow and conductive heat transfer accelerate permafrost degradation. Some of the speculations suggested that these factors can be equally important as climate warming progresses. The prediction of future consequences of climate change is very difficult due to the complexity of ongoing processes in the permafrost environment. The tools and knowledge currently used to evaluate the mutual interactions between the permafrost area and climate change must be continuously verified and improved. More sophisticated computational simulations are needed and some of them are already accessible to implement all the factors influencing groundwater flow, permafrost dynamics, and climate warming (Painter et al., 2016). Moreover, although the scientists argued over the importance of various heat transport mechanisms in continuous and discontinuous regions, there is no doubt that all of them contributed to a greater or lesser degree of permafrost degradation. To improve our understanding of the dependencies that exist between permafrost thaw and groundwater flow, more studies should combine energy and water transport with the enthalpy of fusion. For prediction, future dynamic changes in the heat transfer in the permafrost region due to conduction, convection, and advection (mass transfer) should be considered. Studies should be conducted more systematically in different regions to help further comparisons.

6 Conclusion

In the permafrost regions, we can distinguish three main types of groundwater depending on their location in relation to the permafrost: suprapermafrost, intrapermafrost, and subpermafrost groundwater. These aquifers can be characterised by different compositions due to several factors, such as the depth of the aquifer, the location, the water-rock interaction, and the geological history. The suprapermafrost groundwater chemistry is characterised by low mineralisation, whereas the subpermafrost groundwater chemistry shows higher mineralisation. The intra-permafrost groundwater chemistry was more diversified, but its composition was more similar to subpermafrost groundwater.

The concentrations of, so far, chemical substances differ between various regions and permafrost conditions (continuous/discontinuous) and their connection with various groundwater aquifers.

In the permafrost area, the hills served as a recharge area for groundwater, while the valleys are discharge points.

The suprapermafrost groundwater is predominantly recharged with meteoric water and meltwater by infiltration (discontinuous permafrost zone) or by fractures in rocks (continuous permafrost region). It can also be recharged by rivers through open taliks. In the continuous permafrost zone, the subpermafrost groundwater can be fed by meteoric water, glacial meltwater, surface water and suprapermafrost groundwater merely through taliks. In the QTP as well as in the Arctic region, groundwater recharge is spatially different and depends on many factors such as terrain altitude, type of soil, permafrost condition, and presence of channels.

Furthermore, polygonal tundra with its characteristics features strongly control drainage flow. Degradation of ice-wedge polygons can dramatically alter suprapermafrost groundwater discharge. Aspect ratio and anisotropy strongly influence ice-wedge polygons drainage.

Global warming contributes to a significant reduction in the thickness of the permafrost and the extent of the permafrost in the

area covered by the permafrost in most northern regions. However, the degradation of confining permafrost greatly influences the hydrological systems in the permafrost regions. We can conclude that permafrost thawing increases groundwater flow and results in deepening groundwater flow paths. The whole SGD depends on the thermal state of permafrost, morphological characteristics of the shelf, geological and lithological characteristics, marine forces, and heat transfer. Their contribution can reinforce or lower the SGD. One of the major consequences of groundwater discharge is increased or decreased, depending on the fluxes of nutrients, metals, and gases from a region to land and ocean waters and changes in their physicochemical properties. It is worth mentioning that springs and associated open-system pingos can be significant sources of methane-rich subpermafrost groundwater and deserves more attention.

We identified several knowledge gaps.

- There are no studies that combine hydrogeochemistry, groundwater flow modelling, and solute transport. The role of advective heat transport in the permafrost region is very often neglected, probably also due to shortening the run-time of the simulation. The omission of advective heat transport in the projection of future permafrost degradation is debatable, and several studies highlighted the significance of advective heat transport in permafrost regions.
- The long-term, interdisciplinary *in situ* measurements are lacking, and therefore model predictions are site specific and limited.
- We recommend more studies on springs and open-system pingos, as they can be significant sources of greenhouse gases.

Future studies should answer the following questions.

- How can the sampling procedure and measurement technique be developed to improve comparison of spatial and temporal groundwater composition in different regions?
- How can groundwater recharge rate and water balance be impacted by ongoing and future permafrost degradation?
- What are the ecological and toxicological threats of alterations in groundwater recharge and discharge in permafrost areas to the environment and human health?
- How will progressive degradation of perennially frozen ground influence the water balance and chemical composition of groundwater in relation to the climate warming effect?
- How can SGD contribute to the amplification of the global warming effect by the potential long-term release of methane into the environment?

Author contributions

MD: Conceptualization, Investigation, Supervision, Writing–original draft. MB: Writing–review and editing. CE: Writing–review and editing. W-LH: Writing–review and editing. MK: Writing–review and editing. LK: Writing–review and editing. KK-M: Visualization and editing. KK: Funding acquisition, Writing–review and editing. AL: Writing–review and editing. PM: Visualization and editing. AS: Writing–review and editing. AW: Visualization and editing. MS: Writing–review and editing. BS: Writing–original draft, Writing–review and editing, Conceptualization, Funding acquisition.

Funding

The authors declare financial support was received for the research, authorship, and/or publication of this article. The research leading to these results has received funding from the Norwegian Financial Mechanism 2014–2021 project no. 2019/34/H/ST10/00645 and 2019/34/H/ST10/00504. In addition, the present study is financed by statutory activities of Institute of Oceanology Polish Academy of Science and National Science Centre project no. 2019/34/E/ST10/00167.

Acknowledgments

We thank Laura Bromboszcz and Piotr Prusiński for the technical support.

Conflict of interest

The authors declare that the research was conducted in the absence of any commercial or financial relationships that could be construed as a potential conflict of interest.

Publisher's note

References

Alexeev, S. V., and Alexeeva, L. P. (2003). Hydrogeochemistry of the permafrost zone in the central part of the yakutian diamond-bearing province, Russia. *Hydrogeol. J.* 11 (5), 574–581. doi:10.1007/s10040-003-0270-8

Andersen, D. T., Pollard, W. H., McKay, C. P., and Heldmann, J. L. (2002). Cold springs in permafrost on earth and mars. *J. Geophys. Res.* 107, 5015. doi:10.1029/2000je001436

Bense, V. F., Ferguson, G., and Kooi, H. (2009). Evolution of shallow groundwater flow systems in areas of degrading permafrost. *Geophys. Res. Lett.* 36, L22401. doi:10.1029/2009gl039225

Bense, V. F., Kooi, H., Ferguson, G., and Read, T. (2012). Permafrost degradation as a control on hydrogeological regime shifts in a warming climate. *J. Geophys. Res.* 117, F03036. doi:10.1029/2011JF002143

Bhatti, A. Z., Farooque, A. A., Li, Q., Abbas, F., and Acharya, B. (2021). Spatial distribution and sustainability implications of the Canadian groundwater resources under changing climate. *Sustainability* 13, 9778. doi:10.3390/su13179778

Bibi, S., Wang, L., Li, X., Zhang, X., and Chen, D. (2019). Response of groundwater storage and recharge in the qaidam basin (Tibetan plateau) to climate variations from 2002 to 2016. *J. Geophys. Res.-Atmos.* 124, 9918–9934. doi:10.1029/2019JD030411

Boike, J., Kattenstroth, B., Abramova, K., Bornemann, N., Chetverova, A., Fedorova, I., et al. (2012). Baseline characteristics of climate, permafrost, and land cover from a new permafrost observatory in the Lena River Delta, Siberia (1998– 2011). *Biogeosciences Discuss.* 9 (10), 13627. doi:10.5194/bgd-9-13627-2012

Böttcher, M. E., Mallast, U., Massmann, G., Moosdorf, N., Müller-Petke, M., and Waska, H. (2023). "Coastal-Groundwater interfaces (submarine groundwater discharge)," in *Ecohydrological interfaces*. Editor S. Krause, et al. (Hoboken, NJ, USA: Wiley Science).

Boulding, J. R., and Ginn, J. S. (2016). *Practical handbook of soil, vadose zone, and groundwater contamination: assessment, prevention, and remediation*. Boca Raton, FL, United States: CRC Press.

Box, J. E., Colgan, W. T., Christensen, T. R., Schmidt, N. M., Lund, M., Parmentier, F.-J. W., et al. (2019). Key indicators of Arctic climate change: 1971–2017. *Environ. Res. Lett.* 14, 045010. doi:10.1088/1748-9326/aafc1b

Bring, A., Fedorova, I., Dibike, Y., Hinzman, L., Mård, J., Mernild, S. H., et al. (2016). Arctic terrestrial hydrology: a synthesis of processes, regional effects, and research challenges. *J. Geophys. Res. Biogeosciences* 121 (3), 621–649. doi:10.1002/2015jg003131

Burke, S. A., Wik, M., Lang, A., Contosta, A. R., Palace, M., Crill, P. M., et al. (2019). Long-term measurements of methane ebullition from thaw ponds. *J. Geophys. Res.-Biogeosci.* 124, 2208–2221. doi:10.1029/2018JG004786

Burnett, W., Bokuniewicz, H., Huettel, M., Moore, W., and Taniguchi, M. (2003). Groundwater and pore water inputs to the coastal zone. *Biogeochemistry* 66, 3–33. doi:10.1023/b:biog.0000006066.21240.53

Celico, P. (1986). *Prospezioni idrogeologiche*. Napoli: Liguori editore.

Charkin, A. N., Rutgers van der Loeff, M., Shakhova, N. E., Gustafsson, Ö., Dudarev, O. V., Cherepnev, M. S., et al. (2017). Discovery and characterization of submarine groundwater discharge in the Siberian Arctic seas: a case study in the Buor-Khaya Gulf, Laptev Sea. *Cryosphere* 11, 2305–2327. doi:10.5194/tc-11-2305-2017

Chen, J., Wu, Y., O'Connor, M., Bayani Cardenas, M., Schaefer, K., Michaelides, R., et al. (2020). Active layer freeze-thaw and water storage dynamics in permafrost environments inferred from InSAR. *Remote. Sens. Environ.* 248, 112007. doi:10.1016/j.rse.2020.112007

Cheng, G., and Jin, H. (2013). Permafrost and groundwater on the Qinghai-Tibet Plateau and in northeast China. *Hydrogeol. J.* 21, 5–23. doi:10.1007/s10040-012-0927-2

Christensen, T. R., and Cox, P. (1995). Response of methane emission from arctic tundra to climatic change: results from a model simulation. *Tellus B* 47, 301–309. doi:10.3402/tellusb.v47i3.16049

Church, T. M. (1996). An underground route for the water cycle. *Nature* 380 (6575), 579–580. doi:10.1038/380579a0

Clark, I. D., Lauriol, B., Harwood, L., and Marschner, M. (2001). Groundwater contributions to discharge in a permafrost setting, big fish river, NWT, Canada. *Arct. Antarct. Alp. Res.* 33, 62–69. doi:10.1080/15230430.2001.12003405

Clilverd, H. M., White, D. M., Tidwell, A. C., and Rawlins, M. A. (2011). The sensitivity of northern groundwater recharge to climate change: a case study in northwest Alaska 1. *JAWRA J. Am. Water Resour. Assoc.* 47 (6), 1228–1240. doi:10.1111/j.1752-1688.2011.00569.x

Cochand, M., Molson, J., Barth, J. A. C., van Geldern, R., Lemieux, J.-M., Fortier, R., et al. (2020). Rapid groundwater recharge dynamics determined from hydrogeochemical and isotope data in a small permafrost watershed near Umiujaq (nunavik, Canada). *Hydrogeol. J.* 28, 853–868. doi:10.1007/s10040-020-02109-x

Connolly, C. T., Cardenas, M. B., Burkart, G. A., Spencer, R. G. M., and McClelland, J. W. (2020). Groundwater as a major source of dissolved organic matter to Arctic coastal waters. *Nat. Commun.* 11, 1479. doi:10.1038/s41467-020-15250-8

Cooper, R. J., Wadham, J. L., Tranter, M., Hodgkins, R., and Peters, N. E. (2002). Groundwater hydrochemistry in the active layer of the proglacial zone, finsterwalderbreen, svalbard. *J. Hydrol.* 269, 208–223. doi:10.1016/S0022-1694(02)00279-2

Creed, I. F., Bergström, A. K., Trick, C. G., Grimm, N. B., Hessen, D. O., Karlsson, J., et al. (2018). Global change-driven effects on dissolved organic matter composition: implications for food webs of northern lakes. *Glob. change Biol.* 24 (8), 3692–3714. doi:10.1111/gcb.14129

Crites, H., Kokelj, S. V., and Lacelle, D. (2020). Icings and groundwater conditions in permafrost catchments of northwestern Canada. *Sci. Rep.* 10, 3283. doi:10.1038/s41598-020-60322-w

Dabrowski, J. S., Charette, M. A., Mann, P. J., Ludwig, S. M., Natali, S. M., Holmes, R. M., et al. (2020). Using radon to quantify groundwater discharge and methane fluxes to a shallow, tundra lake on the yukon-kuskokwim delta, Alaska. *Biogeochemistry* 148, 69–89. doi:10.1007/s10533-020-00647-w

Dagenais, S., Lemieux, J.-M., Fortier, R., and Therrien, R. (2020). Coupled cryo-hydrogeological modelling of permafrost dynamics near Umiujaq (nunavik, Canada). *Hydrogeol. J.* 28, 887–904. doi:10.1007/s10040-020-02111-3

DeFoor, W., Person, M., Larsen, H. C., Lizarralde, D., Cohen, D., and Dugan, B. (2011). Ice sheet–derived submarine groundwater discharge on Greenland's continental shelf. *Water Resour. Res.* 47 (7), 536. doi:10.1029/2011wr010536

Dhungel, R., Allen, R. G., Trezza, R., and Robison, C. W. (2016). Evapotranspiration between satellite overpasses: methodology and case study in agricultural dominant semi-arid areas. *Mater. Apps* 23, 714–730. doi:10.1002/met.1596

Dimova, N. T., Paytan, A., Kessler, J. D., Sparrow, K. J., Kodovska, F.G.-T., Lecher, A. L., et al. (2015). Current magnitude and mechanisms of groundwater discharge in the arctic: case study from Alaska. *Environ. Sci. Technol.* 49, 12036–12043. doi:10.1021/acs.est.5b02215

Dobinski, W. (2011). Permafrost. *Earth-Science Rev.* 108 (3-4), 158–169. doi:10.1016/j.earscirev.2011.06.007

Döll, P., and Fiedler, K. (2008). Global-scale modeling of groundwater recharge. *Hydrol. Earth Syst. Sci.* 12 (3), 863–885. doi:10.5194/hess-12-863-2008

Doloisio, N., and Vanderlinden, J. P. (2020). The perception of permafrost thaw in the Sakha Republic (Russia): narratives, culture and risk in the face of climate change. *Polar Sci.* 26, 100589. doi:10.1016/j.polar.2020.100589

Dragon, K., and Marciniak, M. (2010). Chemical composition of groundwater and surface water in the Arctic environment (Petuniabukta region, central Spitsbergen). *J. Hydrol.* 386, 160–172. doi:10.1016/j.jhydrol.2010.03.017

Dugan, H. A., Gleeson, T., Lamoureux, S. F., and Novakowski, K. (2012). Tracing groundwater discharge in a High Arctic lake using radon-222. *Environ. earth Sci.* 66, 1385–1392. doi:10.1007/s12665-011-1348-6

Ensom, T., Makarieva, O., Morse, P., Kane, D., Alekseev, V., and Marsh, P. (2020). The distribution and dynamics of aufeis in permafrost regions. *Permafr. Periglac. Process.* 31 (3), 383–395. doi:10.1002/ppp.2051

Evans, S. G., and Ge, S. (2017). Contrasting hydrogeologic responses to warming in permafrost and seasonally frozen ground hillslopes Geophys. *Res. Lett.* 44, 2016GL072009. doi:10.1002/2016GL072009

Evans, S. G., Ge, S., Voss, C. I., and Molotch, N. P. (2018). The role of frozen soil in groundwater discharge predictions for warming alpine watersheds Water Resour. *Res.* 54, 1599–1615. doi:10.1002/2017WR022098

Everdingen, R. V. (1998). *Glossary of permafrost and related ground-ice terms*. Washington, D. C., USA: National Research Council of the National Academies, 2550.

Flohn, H. (1980). Possible climatic consequences of a man-made global warming. https://core.ac.uk/download/pdf/33893066.pdf.

Frampton, A., Painter, S. L., and Destouni, G. (2013). Permafrost degradation and subsurface-flow changes caused by surface warming trends. *Hydrol. J.* 21, 271–280. doi:10.1007/s10040-012-0938-z

Frey, K. E., Siegel, D. I., and Smith, L. C. (2007). Geochemistry of west Siberian streams and their potential response to permafrost degradation. *Water Resour. Res.* 43, W03406. doi:10.1029/2006WR004902

Gao, Bo, and Coon, E. T. (2022). Evaluating simplifications of subsurface process representations for field-scale permafrost hydrology models. *Cryosphere* 16 (10), 4141–4162. doi:10.5194/tc-16-4141-2022

Ge, S., McKenzie, J. M., Voss, C. I., and Wu, Q. (2011). Exchange of groundwater and surfacewater mediated by permafrost response to seasonal and long term air temperature variation. *Geophys. Res. Lett.* 38 (14), L14402. doi:10.1029/2011gl047911

Ghias, M. S., Therrien, R., Molson, J., and Lemieux, J.-M. (2017). Controls on permafrost thaw in a coupled groundwater-flow and heat-transport system: iqaluit airport, nunavut, Canada. *Hydrogeol. J.* 25, 657–673. doi:10.1007/s10040-016-1515-7

Grasby, S. E., Beauchamp, B., and Bense, V. (2012). Sulfuric acid speleogenesis associated with a glacially driven groundwater system—paleo-spring "pipes" at borup fiord pass, nunavut. *Nunavut, Astrobiol.* 12, 19–28. doi:10.1089/ast.2011.0700

Green, T. R., Taniguchi, M., Kooi, H., Gurdak, J. J., Allen, D. M., Hiscock, K. M., et al. (2011). Beneath the surface of global change: impacts of climate change on groundwater. *J. Hydrology* 405 (3-4), 532–560. doi:10.1016/j.jhydrol.2011.05.002

Guimond, J. A., Mohammed, A. A., Walvoord, M. A., Bense, V. F., and Kurylyk, B. L. (2022). Sea-level rise and warming mediate coastal groundwater discharge in the Arctic. *Environ. Res. Lett.* 17 (4), 045027. doi:10.1088/1748-9326/ac6085

Haldorsen, S., Heim, M., Dale, B., Landvik, J. Y., van der Ploeg, M., Leijnse, A., et al. (2010). Sensitivity to long-term climate change of subpermafrost groundwater systems in svalbard. *Quat. Res.* 73, 393–402. doi:10.1016/j.yqres.2009.11.002

Haldorsen, S., Heim, M., and Lauritzen, S. E. (1996). Subpermafrost groundwater, western svalbard. *Hydrol* 27, 57–68. doi:10.2166/nh.1996.0019

Haldorsen, S., Heim, M., and van der Ploeg, M. (2011). "Impacts of climate change on groundwater in permafrost areas: case study from svalbard, Norway," in *Climate change effects on groundwater resources: a global synthesis of findings and recommendations*. Editor H. Treidel, et al. (Wallington, UK: CRC Press), 323–340.

Harp, D. R., Zlotnik, V., Abolt, C. J., Newman, B. D., Atchley, A. L., Jafarov, E., et al. (2020). New insights into the drainage of inundated Arctic polygonal tundra using fundamental hydrologic principles. *Cryosphere Discuss.*, 1–26. doi:10.5194/tc-2020-100

Hart, P. E., Pohlman, J. W., Lorenson, T. D., and Edwards, B. D. (2011). "Beaufort Sea Deep-water gas hydrate recovery from a seafloor mound in a region of widespread BSR occurrence," in *Proceedings of the 7th international conference on gas hydrates (ICGH 2011)* (Edinburgh, Scotland: ICGH).

Hawkswell, J. (2018). Characterizing ice-wedge polygon geomorphology in the haughton impact structure, devon island. Doctoral dissertation. Canada: The University of Western Ontario.

Hay, A. E. (1984). Remote acoustic imaging of the plume from a submarine spring in an Arctic fjord. *Science* 225 (4667), 1154–1156. doi:10.1126/science.225.4667.1154

Helbig, M., Boike, J., Langer, M., Schreiber, P., Runkle, B. R., and Kutzbach, L. (2013). Spatial and seasonal variability of polygonal tundra water balance: Lena River Delta, northern Siberia (Russia). *Hydrogeol. J.* 21 (1), 133–147. doi:10.1007/s10040-012-0933-4

Herczeg, A. L., and Edmunds, W. M. (2000). "Inorganic ions as tracers," in *Environmental tracers in subsurface hydrology*. Editors P. G. Cook and A. L. Herczeg (Boston, MA, USA: Springer). doi:10.1007/978-1-4615-4557-6_2

Hinzman, L. D., Bettez, N. D., Bolton, W. R., Chapin, F. S., Dyurgerov, M. B., Fastie, C. L., et al. (2005). Evidence and implications of recent climate change in northern Alaska and other arctic regions. *Clim. change* 72, 251–298. doi:10.1007/s10584-005-5352-2

Hodson, A. J., Nowak, A., Hornum, M. T., Senger, K., Redeker, K., Christiansen, H. H., et al. (2020). Sub-permafrost methane seepage from open-system pingos in Svalbard. *Cryosphere* 14 (11), 3829–3842. doi:10.5194/tc-14-3829-2020

Hodson, A. J., Nowak, A., Redeker, K. R., Holmlund, E. S., Christiansen, H. H., and Turchyn, A. V. (2019). Seasonal dynamics of methane and carbon dioxide evasion from an open system pingo: lagoon pingo, Svalbard. *Front. Earth Sci.* 7, 30. doi:10.3389/feart.2019.00030

Holgerson, M. A. (2015). Drivers of carbon dioxide and methane supersaturation in small, temporary ponds. *Biogeochemistry* 124, 305–318. doi:10.1007/s10533-015-0099-y

Hong, W.-L., Lepland, A., Himmler, T., Kim, J.-H., Chand, S., Sahy, D., et al. (2019). Discharge of meteoric water in the eastern Norwegian Sea since the last glacial period. *Geophys. Res. Lett.* 46, 8194–8204. doi:10.1029/2019GL084237

Hu, R., Liu, Q., and Xing, Y. (2018). Case study of heat transfer during artificial ground freezing with groundwater flow. *Water* 10, 1322. doi:10.3390/w10101322

Hu, Y., Ma, R., Wang, Y., Chang, Q., Wang, S., Ge, M., et al. (2019). Using hydrogeochemical data to trace groundwater flow paths in a cold alpine catchment. *Hydrol. Process* 33, 1942–1960. doi:10.1002/hyp.13440

Immerzeel, W. W., Van Beek, L. P., and Bierkens, M. F. (2010). Climate change will affect the Asian water towers. *science* 328 (5984), 1382–1385. doi:10.1126/science.1183188

Ireson, A., van der Kamp, G., Ferguson, N. U., Nachshon, U., and Wheater, H. S. (2013). Hydrogeological processes in seasonally frozen northern latitudes: understanding, gaps and challenges. *Hydrogeology J.* 21, 53–66. doi:10.1007/s10040-012-0916-5

Jamin, P., Cochand, M., Dagenais, S., Lemieux, J.-M., Fortier, R., Molson, J., et al. (2020). Direct measurement of groundwater flux in aquifers within the discontinuous permafrost zone: an application of the finite volume point dilution method near Umiujaq (nunavik, Canada). *Hydrogeol. J.* 28, 869–885. doi:10.1007/s10040-020-02108-y

Jia, W., Meibing, J., Takahashi, J., Suzuki, T., Polyakov, I. V., Mizobata, K., et al. 1958. Modeling Arctic Ocean heat transport and warming episodes in the 20th century caused by the intruding Atlantic Water. 极地研究, 19p.159.

Jin, H., He, R., Cheng, G., Wu, Q., Wang, S., Lü, L., et al. (2009). Changes in frozen ground in the source area of the yellow river on the Qinghai-Tibet Plateau, China, and their eco-environmental impacts. *Environ. Res. Lett.* 4, 045206. doi:10.1088/1748-9326/4/4/045206

Jorgenson, M. T., Racine, C. H., Walters, J. C., and Osterkamp, T. E. (2001). Permafrost degradation and ecological changes associated with a warming climate in central Alaska. *Clim. Change.* 48, 551–579. doi:10.1023/A:1005667424292

Kane, D. L., Yoshikawa, K., and McNamara, J. P. (2013). Regional groundwater flow in an area mapped as continuous permafrost, NE Alaska (USA). *Hydrogeol. J.* 21, 41–52. doi:10.1007/s10040-012-0937-0

Kendrick, M. R., Huryn, A. D., Bowden, W. B., Deegan, L. A., Findlay, R. H., Hershey, A. E., et al. (2018). Linking permafrost thaw to shifting biogeochemistry and food web resources in an arctic river. *Glob. Change Biol.* 24 (12), 5738–5750. doi:10.1111/gcb.14448

Khare, N., and Khare, R. (1968). *The arctic*. Boca Raton, Florida, United States: CRC Press.

Kies, A., Nawrot, A., Tosheva, Z., and Jania, J. (2011). Natural radioactive isotopes in glacier meltwater studies. *Geochem. J.* 45 (6), 423–429. doi:10.2343/geochemj.1.0141

Kim, J.-H., Ryu, J.-S., Hong, W.-L., Jang, K., Joo, Y. J., Lemarchand, D., et al. (2022). Assessing the impact of freshwater discharge on the fluid chemistry in the Svalbard fjords. *Sci. Total. Environ.* 835, 155516. doi:10.1016/j.scitotenv.2022.155516

Kleber, M., Bourg, I. C., Coward, E. K., Hansel, C. M., Myneni, S. C. B., and Nunan, N. (2021). Dynamic interactions at the mineral–organic matter interface. *Nat. Rev. Earth Environ.* 2, 402–421. doi:10.1038/s43017-021-00162-y

Kong, F., Sha, Z., Luo, X., Du, J., Jiao, J. J., Moore, W. S., et al. (2019). Evaluation of lacustrine groundwater discharge and associated nutrients, trace elements and DIC loadings into Qinghai Lake in Qinghai-Tibetan Plateau, using radium isotopes and hydrological methods. *Chem. Geol.* 510, 31–46. doi:10.1016/j.chemgeo.2019.01.020

Kuhn, M., Lundin, E. J., Giesler, R., Johansson, M., and Karlsson, J. (2018). Emissions from thaw ponds largely offset the carbon sink of northern permafrost wetlands. *Sci. Rep.* 8, 9535. doi:10.1038/s41598-018-27770-x

Lamontagne-Hallé, P., McKenzie, J. M., Kurylyk, B. L., and Zipper, S. C. (2018). Changing groundwater discharge dynamics in permafrost regions. *Environ. Res. Lett.* 13, 084017. doi:10.1088/1748-9326/aad404

Larsen, J. N., Schweitzer, P., Abass, K., Doloisio, N., Gartler, S., Ingeman-Nielsen, T., et al. (2021). Thawing permafrost in Arctic coastal communities: a framework for studying risks from climate change. *Sustainability* 13 (5), 2651. doi:10.3390/su13052651

Lecher, A. L., Chien, C.-T., and Paytan, A. (2016a). Submarine groundwater discharge as a source of nutrients to the north pacific and arctic coastal ocean. *Mar. Chem.* 186, 167–177. doi:10.1016/j.marchem.2016.09.008

Lecher, A. L., Kessler, J., Sparrow, K., Garcia-Tigreros Kodovska, F., Dimova, N., Murray, J., et al. (2016b). Methane transport through submarine groundwater discharge to the North Pacific and Arctic Ocean at two Alaskan sites. *Limnol. Oceanogr.* 61, S344–S355. doi:10.1002/lno.10118

Lehmann, N., Lantuit, H., Böttcher, M. E., Hartmann, J., Eulenburg, A., and Thomas, H. (2023). Alkalinity generation from carbonate weathering in a silicate-dominated headwater catchment at Iskorasfjellet, northern Norway. *Biogeosciences* 2 (16), 3459–3479. doi:10.5194/bg-20-3459-2023

Liao, Z. (2018). *Thermal springs and geothermal energy in the Qinghai-Tibetan plateau and the surroundings*. Berlin, Germany: Springer. doi:10.1007/978-981-10-3485-5

Liljedahl, A., Boike, J., Daanen, R., Fedorov, A. N., Frost, G. V., Grosse, G., et al. (2016). Pan-Arctic ice-wedge degradation in warming permafrost and its influence on tundra hydrology. *Nat. Geosci.* 9, 312–318. doi:10.1038/ngeo2674

Liljedahl, A. K., Hinzman, L. D., and Schulla, J. (2012). "Ice-wedge polygon type controls low-gradient watershed-scale hydrology," in Proceedings of the Tenth International Conference on Permafrost, Russia, June, 2012.

Luijendijk, E., Gleeson, T., and Moosdorf, N. (2020). Fresh groundwater discharge insignificant for the world's oceans but important for coastal ecosystems. *Nat. Commun.* 11, 1260. doi:10.1038/s41467-020-15064-8

Luo, J., Niu, F., Lin, Z., Liu, M., and Yin, G. (2019). Recent acceleration of thaw slumping in permafrost terrain of Qinghai-Tibet Plateau: an example from the Beiluhe Region. *Geomorphology* 341, 79–85. doi:10.1016/j.geomorph.2019.05.020

Luo, X., Kuang, X., Jiao, J. J., Liang, S., Mao, R., Zhang, X., et al. (2018). Evaluation of lacustrine groundwater discharge, hydrologic partitioning, and nutrient budgets in a proglacial lake in the Qinghai–Tibet Plateau: using ²²²Rn and stable isotopes. *Hydrology Earth Syst. Sci.* 22 (10), 5579–5598. doi:10.5194/hess-22-5579-2018

Ma, R., Sun, Z., Hu, Y., Chang, Q., Wang, S., Xing, W., et al. (2017). Hydrological connectivity from glaciers to rivers in the Qinghai–Tibet Plateau: roles of suprapermafrost and subpermafrost groundwater. *Hydrol. Earth Syst. Sci.* 21, 4803–4823. doi:10.5194/hess-21-4803-2017

MacDonald, G. J. (1990). Role of methane clathrates in past and future climates. *Clim. Change.* 16, 247–281. doi:10.1007/BF00144504

Malov, A. I. (2021). Tritium records to trace groundwater recharge and mixing in the western Russian Arctic. *Environ. Earth Sci.* 80, 583. doi:10.1007/s12665-021-09893-z

Manabe, S., Stouffer, R. J., Spelman, M. J., and Bryan, K. (1991). Transientresponses of a coupled ocean-atmosphere model to gradual changesof atmospheric CO2. Part I: annual mean response. *J. ofClimate4* 4, 785–818. doi:10.1175/1520-0442(1991)004<0785:troaco>2.0.co;2

Manasypov, R. M., Lim, A. G., Krickov, I. V., Shirokova, L. S., Vorobyev, S. N., Kirpotin, S. N., et al. (2020). Spatial and seasonal variations of C, nutrient, and metal concentration in thermokarst lakes of Western Siberia across a permafrost gradient. *Water* 12 (6), 1830. doi:10.3390/w12061830

Marszałek, H., and Wąsik, M. (2013). Some physico-chemical features of water in suprapermafrost zone in the Hornsund region (SW spitsbergen). *Biul. Państwowego Inst. Geol.* 456, 397–404.

McBean, G., Alekseev, G., Chen, D., Førland, E., Fyfe, J., Groisman, P., et al. (2005). "Arctic climate: past and present," in *Arctic climate mpact assessment*. Editors C. Symon, L. Arris, and B. Heal (Cambridge, UK: Cambridge University Press), 21–60.

McKenzie, J. M., and Voss, C. I. (2013). Permafrost thaw in a nested groundwater-flow system. *Hydrogeology J.* 21 (1), 299–316. doi:10.1007/s10040-012-0942-3

Michael, H. A. (2005). *Seasonal dynamics in costal aquifers: investigation of submarine groundwater discharge through field measurements and numerical models*. Doctoral dissertation. Cambridge, MA, USA: Massachusetts Institute of Technology.

Michel, F. A., and van Everdingen, R. O. (1994). Changes in hydrogeologic regimes in permafrost regions due to climatic change. *Permafr. Periglac.* 5, 191–195. doi:10.1002/ppp.3430050308

Mohammed, A. A., Bense, V. F., Kurylyk, B. L., Jamieson, R. C., Johnston, L. H., and Jackson, A. J. (2021). Modeling reactive solute transport in permafrost-affected groundwater systems. *Water Resour. Res.* 57, e2020WR028771. doi:10.1029/2020WR028771

Moore, W. S. (2010). The effect of submarine groundwater discharge on the ocean. *Annu. Rev. Mar. Sci.* 2, 59–88. doi:10.1146/annurev-marine-120308-081019

Moosdorf, N., Böttcher, M. E., Adyasari, D., Erkul, E., Gilfedder, B., Greskowiak, J., et al. 2021. A state-of-the-art perspective on the characterization of subterranean estuaries at the regional scale. *Front. Earth Sci.* 9, 601293, 1–26. doi:10.3389/feart.2021.601293

Nitzbon, J., Westermann, S., Langer, M., Martin, L. C. P., Strauss, J., Laboor, S., et al. (2020). Fast response of cold ice-rich permafrost in northeast Siberia to a warming climate. *Nat. Commun.* 11, 2201. doi:10.1038/s41467-020-15725-8

Obu, J. (2021). How much of the earth's surface is underlain by permafrost? *J. Geophys. Res. Earth Surf.* 126 (5), e2021JF006123. doi:10.1029/2021jf006123

O'Donnell, J. A., Aiken, G. R., Walvoord, M. A., and Butler, K. D. (2012). Dissolved organic matter composition of winter flow in the Yukon River basin: implications of permafrost thaw and increased groundwater discharge. *Glob. Biogeochem. Cycles* 26 (4). doi:10.1029/2012gb004341

Oechel, W. C., Vourlitis, G. L., Hastings, S. J., Zulueta, R. C., Hinzman, L., and Kane, D. (2000). Acclimation of ecosystem CO2 exchange in the Alaskan Arctic in response to decadal climate warming. *Nature* 406, 978–981. doi:10.1038/35023137

Olichwer, T., Tarka, R., and Modelska, M. (2013). Chemical composition of groundwaters in the Hornsund region, southern Spitsbergen. *South. Spitsb. Hydrol. Res.* 44, 117–130. doi:10.2166/nh.2012.075

Olid, C., Zannella, A., and Lau, D. C. P. (2021). The role of methane transport from the active layer in sustaining methane emissions and food chains in subarctic ponds. *J. Geophys. Res.-Biogeo.* 126, e2020JG005810. doi:10.1029/2020JG005810

Omelon, C. R., Pollard, W. H., and Marion, G. M. (2001). Seasonal formation of ikaite (CaCO3 6H2O) in saline spring discharge at Expedition Fiord, Canadian High Arctic: assessing conditional constraints for natural crystal growth. *Geochimica Cosmochimica Acta* 65, 1429–1437. doi:10.1016/s0016-7037(00)00620-7

Painter, S. L., Coon, E. T., Atchley, A. L., Berndt, M., Garimella, R., Moulton, J. D., et al. (2016). Integrated surface/subsurface permafrost thermal hydrology: model formulation and proof-of-concept simulations. *Water Resour. Res.* 52 (8), 6062–6077. doi:10.1002/2015wr018427

Painter, S. L., Coon, E. T., Khattak, A. J., and Jastrow, J. D. (2023). Drying of tundra landscapes will limit subsidence-induced acceleration of permafrost thaw. *Proc. Natl. Acad. Sci.* 120 (8), e2212171120. doi:10.1073/pnas.2212171120

Pan, X., Yu, Q., You, Y., Chun, K. P., Shi, X., and Li, Y. (2017). Contribution of supra-permafrost discharge to thermokarst lake water balances on the northeastern Qinghai-Tibet Plateau. *J. Hydrology* 555, 621–630. doi:10.1016/j.jhydrol.2017.10.046

Paull, C. K., Dallimore, S. R., Caress, D. W., Gwiazda, R., Melling, H., Riedel, M., et al. (2015). Active mud volcanoes on the continental slope of the C anadian B eaufort S ea. *Geochem. Geophys. Geosystems* 16 (9), 3160–3181. doi:10.1002/2015gc005928

Paull, C. K., Dallimore, S. R., Jin, Y. K., Caress, D. W., Lundsten, E., Gwiazda, R., et al. (2022). Rapid seafloor changes associated with the degradation of Arctic submarine permafrost. *Proc. Natl. Acad. Sci.* 119 (12), e2119105119. doi:10.1073/pnas.2119105119

Pavlova, N., Ogonerov, V., Danzanova, M., and Popov, V. (2020). Hydrogeology of reclaimed floodplain in a permafrost area, yakutsk, Russia. *Geosciences* 10 (5), 192. doi:10.3390/geosciences10050192

Pavlova, N. A., Kolesnikov, A. B., Efremov, V. S., and Shepelev, V. V. (2016). Groundwater chemistry in intrapermafrost taliks in central Yakutia. *Water Resour.* 43, 353–363. doi:10.1134/S0097807816020135

Paytan, A., Lecher, A. L., Dimova, N., Sparrow, K. J., Kodovska, F. G., Murray, J., et al. (2015). Methane transport from the active layer to lakes in the Arctic using Toolik Lake, Alaska, as a case study. *Proc. Natl. Acad. Sci.* 112 (12), 3636–3640. doi:10.1073/pnas.1417392112

Pokrovsky, O. S., Manasypov, R. M., Loiko, S., Shirokova, L. S., Krickov, I. A., Pokrovsky, B. G., et al. (2015). Permafrost coverage, watershed area and season control of dissolved carbon and major elements in western Siberian rivers. *Biogeosciences* 12 (21), 6301–6320. doi:10.5194/bg-12-6301-2015

Pollard, W., Omelon, C., Andersen, D., and McKay, C. (1999). Perennial spring occurrence in the expedition fiord area of western Axel Heiberg Island, Canadian high arctic. *Can. J. Earth Sci.* 36 (1), 105–120. doi:10.1139/e98-097

Pollard, W. H. (1991). "A High Arctic occurrence of seasonal frost mounds," in *Proceedings, northern hydrology symposium, environment*. Editors T. Prowse and C. Ommanney (Saskatoon, Canada: National Human Rights Institutions).

Pollard, W. H. (2005). Icing processes associated with high arctic perennial springs, Axel Heiberg Island, nunavut, Canada. *Permafr. Periglac. Process.* 16, 51–68. doi:10.1002/ppp.515

Pollard, W. H., and French, H. M. (1984). The groundwater hydraulics of seasonal frost mounds, North Fork Pass, Yukon Territory. *Can. J. Earth Sci.* 21 (10), 1073–1081. doi:10.1139/e84-112

Rowland, J. C., Jones, C. E., Altmann, G., Bryan, R., Crosby, B. T., Hinzman, L. D., et al. (2010). Arctic landscapes in transition: responses to thawing permafrost. *Eos, Trans. Am. Geophys. Union* 91 (26), 229–230. doi:10.1029/2010eo260001

Rowland, J. C., Travis, B. J., and Wilson, C. J. (2011). The role of advective heat transport in talik development beneath lakes and ponds in discontinuous permafrost. *Geophys. Res. Lett.* 38, L17504. doi:10.1029/2011GL048497

Ruppel, C. (2015). Permafrost-associated gas hydrate: is it really approximately 1% of the global system? *J. Chem. Eng.* 60 (2), 429–436. doi:10.1021/je500770m

Rysiukiewicz, M., Marszałek, H., and Wąsik, M. (2023). Forming of water chemistry in active layer, Steinvik River catchment, SW Spitsbergen. *Pol. Polar Res.* 44. doi:10.24425/ppr.2022.143313

Santos, I. R., Chen, X., Lecher, A. L., Sawyer, A. H., Moosdorf, N., Rodellas, V., et al. (2021). Submarine groundwater discharge impacts on coastal nutrient biogeochemistry. *Nat. Rev. Earth Environ.* 2 (5), 307–323. doi:10.1038/s43017-021-00152-0

Semenov, A., Zhang, X., Rinke, A., Dorn, W., and Dethloff, K. (2019). Arctic intense summer storms and their impacts on sea ice—a regional climate modeling study. *Atmosphere* 10 (4), 218. doi:10.3390/atmos10040218

Scheidegger, J. M. (2013). *Impact of permafrost dynamics on Arctic groundwater flow systems with application to the evolution of spring and lake taliks*. PhD thesis. Norwich, England: School of Environmental Sciences of the University of East Anglia.

Scheidegger, J. M., Bense, V. F., and Grasby, S. E. (2012). Transient nature of Arctic spring systems driven by subglacial meltwater. *Geophys. Res. Lett.* 39, L12405. doi:10.1029/2012GL051445

Schuur, E. A. G., McGuire, A. D., Schädel, C., Grosse, G., Harden, J. W., Hayes, D. J., et al. (2015). Climate change and the permafrost carbon feedback. *Nature* 250, 171–179. doi:10.1038/nature14338

Shakhova, N., Semiletov, I., Leifer, I., Sergienko, V., Salyuk, A., Kosmach, D., et al. (2014). Ebullition and storm-induced methane release from the east Siberian arctic shelf. *Nat. Geosci.* 7 (1), 64–70. doi:10.1038/ngeo2007

Shijin, W., Wenli, Q., and Qiaoxia, L. (2023). Key pathways to achieve sustainable development goals in three polar regions. *Sustainability* 15 (2), 1735. doi:10.3390/su15021735

Sjöberg, Y., Coon, E., Sannel, A. B. K., Pannetier, R., Harp, D., Frampton, A., et al. (2016). Thermal effects of groundwater flow through subarctic fens: a case study based on field observations and numerical modeling. *Water Resour. Res.* 52, 1591–1606. doi:10.1002/2015WR017571

Sjöberg, Y., Jan, A., Painter, S. L., Coon, E. T., Carey, M. P., O'Donnell, J. A., et al. (2021). Permafrost promotes shallow groundwater flow and warmer headwater streams. *Water Resour. Res.* 57 (2), e2020WR027463. doi:10.1029/2020wr027463

Slomp, C. P., and Van Cappellen, P. (2004). Nutrient inputs to the coastal ocean through submarine groundwater discharge: controls and potential impact. *J. Hydrology* 295 (1-4), 64–86. doi:10.1016/j.jhydrol.2004.02.018

Song, C., Wang, G., Mao, T., Chen, X., Huang, K., Sun, X., et al. (2019). Importance of active layer freeze-thaw cycles on the riverine dissolved carbon export on the Qinghai-Tibet Plateau permafrost region. *PeerJ* 7, 71466–e7225. doi:10.7717/peerj.7146

Song, C., Wang, G., Mao, T., Dai, J., and Yang, D. (2020). Linkage between permafrost distribution and river runoff changes across the arctic and the Tibetan plateau. *Sci. China Earth Sci.* 63, 292–302. doi:10.1007/s11430-018-9383-6

Swarzenski, P., Reich, C., Spechler, R., Kindinger, J., and Moore, W. (2001). Using multiple geochemical tracers to characterize the hydrogeology of the submarine spring off Crescent Beach, Florida. *Chem. Geol.* 179 (1-4), 187–202. doi:10.1016/S0009-.2541(01)00322-9

Szymczycha, B., Kłostowska, Ż., Lengier, M., and Dzierzbicka-Głowacka, L. (2020). Significance of nutrient fluxes via submarine groundwater discharge in the Bay of Puck, southern Baltic Sea. *Oceanologia* 62 (2), 117–125. doi:10.1016/j.oceano.2019.12.004

Taniguchi, M., Dulai, H., Burnett, K. M., Santos, I. R., Sugimoto, R., Stieglitz, T., et al. (2019). Submarine groundwater discharge: updates on its measurement techniques, geophysical drivers, magnitudes, and effects. *Front. Environ. Sci.* 7, 141. doi:10.3389/fenvs.2019.00141

Tóth, J. (1999). Groundwater as a geologic agent: an overview of the causes, processes, and manifestations. *Hydrogeol. J.* 7, 1–14. doi:10.1007/s100400050176

Turner, J., Overland, J. E., and Walsh, J. E. (2007). An Arctic and antarctic perspective on recent climate change. *Int. J. Climatol.* 27, 277–293. doi:10.1002/joc.1406

Utting, N., Lauriol, B., Mochnacz, N., Aeschbach-Hertig, W., and Clark, I. (2013). Noble gas and isotope geochemistry in western Canadian Arctic watersheds: tracing groundwater recharge in permafrost terrain. *Hydrogeol. J.* 21, 79–91. doi:10.1007/s10040-012-0913-8

van Everdingen, R. O. (1981). Morphology, hydrology and hydrochemistry of karst in permafrost terrain near Great Bear Lake, N. W. T. *Nat. Hydrol. Res. Inst. Inland Water Dir.* 11, 53.

Van Everdingen, R. O. (1990). "Ground-water hydrology," in *Northern hydrology: Canadian perspectives*. Editors T. D. Prowse and C. S. L. Ommanney (Saskatoon, Canada: National Hydrological Research Institute), 77–101.

van Stempvoort, D. R., Spoelstra, J., Bickerton, G., Koehler, G., Mayer, B., Nightingale, M., et al. (2023). Sulfate in streams and groundwater in a cold region (Yukon Territory, Canada): evidence of weathering processes in a changing climate. *Chem. Geol.* 631, 121510. doi:10.1016/j.chemgeo.2023.121510

Walvoord, M. A., and Kurylyk, B. L. (2016). Hydrologic impacts of thawing permafrost - a review. *Vadose Zone J.* 15, 1–20. doi:10.2136/vzj2016.01.0010

Wang, X., Chen, R., and Yang, Y. (2017). Effects of permafrost degradation on the hydrological regime in the source regions of the Yangtze and yellow rivers, China. *Water* 9, 897. doi:10.3390/w9110897

Washburn, L. L. (1969). Weathering frost action and patterned ground in the Mesters Vig district, Northest Greenland—medd. *Gronland* 176 (303), 20–033.

Wellman, T. P., Voss, C. I., and Walvoord, M. A. (2013). Impacts of climate, lake size, and supra- and sub-permafrost groundwater flow on lake-talik evolution, Yukon flats, Alaska (USA). *Hydrogeol. J.* 21, 281–298. doi:10.1007/s10040-012-0941-4

Williams, J. R. (1970). *GroundWater in the permafrost regions of Alaska, USGS prof*. Reston, VA, USA: US Geological Survey. doi:10.3133/pp696

Woo, M. K. (2011). "Linking runoff to groundwater in permafrost terrain," in *Sustaining groundwater resources. International year of planet Earth*. Editor J. Jones (Dordrecht, Netherlands: Springer). doi:10.1007/978-90-481-3426-7_8

Woo, M. K. (2012). *Permafrost hydrology*. Berlin, Germany: Springer Science & Business Media.

Wu, T., Zhao, L., Li, R., Wang, Q., Xie, C., and Pang, Q. (2013). Recent ground surface warming and its effects on permafrost on the central Qinghai-Tibet Plateau. *Int. J. Climatol.* 33 (4), 920–930. doi:10.1002/joc.3479

Yao, Y., Zheng, C., Liu, J., Cao, G., Xiao, H., Li, H., et al. (2015). Conceptual and numerical models for groundwater flow in an arid inland river basin. *Hydrol. Process.* 29 (6), 1480–1492. doi:10.1002/hyp.10276

Yi, P., Wan, C., Jin, H., Luo, D., Yang, Y., Wang, Q., et al. (2018). Hydrological insights from hydrogen and oxygen isotopes in source area of the yellow river, east-northern part of qinghai–tibet plateau. *J. Radioanalytical Nucl. Chem.* 317, 131–144. doi:10.1007/s10967-018-5864-7

Yoshikawa, K. (1998). "The groundwater hydraulics of open system pingos," in Proceedings of the 7th International Permafrost Conference Yellowknife, Canada, June, 1998, 1177–1183.